Nearshore Ecology (NSE) of Grand Canyon Fish 2011 Progress Report

Report Authors:
Bill Pine, University of Florida, billpine@ufl.edu
Mike Dodrill, University of Florida
Colton Finch, University of Florida
Brandon Gerig, University of Florida
Karin Limburg, State University of New York-ESF

Project Personnel:
UF: Forest Hayes, Jessie Pierson, Jake Hall
SUNY-ESF: T. Hayden
Ecometric: J. Korman

GCMRC Coordinators:
Mike Yard
Scott Vanderkooi

Note: All information presented should be considered draft and subject to revision based on corrections and updates to field data and analytical approaches. This document is prepared as a courtesy to our cooperators. The final report for this project will be presented in 2012.

List of abbreviations

Fish species – Common name

BBH – Black bullhead
BKC – Black crappie
BNT – Brown trout
CCF – Channel catfish
CRP – Common carp
FHM – Fathead minnow
FMS – Flannelmouth sucker
GSF – Green sunfish
HBC – Humpback chub
PKF – Plains killifish
RBT – Rainbow trout
RSH – Red shiner
SPD – Speckled dace
STB – Striped bass
SUC – Unidentified sucker

Places

COR – Colorado River
LCR – Little Colorado River

Gear

EF – Boat electrofishing
HN – Hoopnets

Other

NSE – Nearshore Ecology Project
UF – University of Florida
GCMRC – United States Geological Survey Grand Canyon Monitoring and Research Center
PIT – Passive Integrated Transponder, a tag type that provides a uniquely identifiable id to each fish
VIE – Visible Implant Elastomer, a tag type that provides a batch mark that identifies the trip, gear, and site a fish was collected

Nearshore Ecology Project 2011 Research Progress Report

The NSE project is designed to assess whether juvenile native fish survival and recruitment are influenced by planned flow experiments from Glen Canyon Dam that occurred during September and October 2009-2011. To make this assessment, our research in 2011 was defined by three domains, each informed by 2009 and 2010 sampling and detailed in our original full proposal. Three key areas where this project seeks to fill existing information gaps are:

(1) Evaluating how steady flows influence juvenile native fish growth and survival,
(2) Assess habitat use and movement of juvenile fish in response to steady flows, and
(3) Identify the spatial source of juvenile native fish found in the mainstem.

This report serves as a preliminary presentation of research results from 2011. These results focus on 2011 sampling and analyses for 2011 field efforts and primarily include catch-rate, movement, capture probability, and abundance estimates for juvenile humpback chub (HBC) as well as geochemical water atlas development and assessment of otolith microchemistry techniques. All information presented should be considered draft and subject to revision based on corrections and updates to field data and analytical approaches through collaboration revisions between NSE core research team and GCMRC cooperators. A detailed final report for project years 2009-2011 will be prepared during 2012 as detailed in the original agreement.

2011 Field Conditions and Sampling Overview

Our sampling universe covered an area from Heart Island (just downstream of the Little Colorado River confluence, Figure 1) to an area just upstream of Lava Chuar rapid (about RM 65.5). Within this sampling universe, we established three sampling sites (Sites 1, 2, and 3) of approximately equal length (about 1500-m) with similar hydrologic features. Each Site was then subdivided further into individual spatially referenced 25-m shoreline segments (“habitat sub-unit”, HSU). We used slow-speed

boat electrofishing (~9 seconds/m of shoreline) during night time to survey each site, broken down into samples covering two consecutive HSUs (50 m total). Fish captured in each sample were placed in a numbered bucket corresponding to the HSUs to track catch spatially by HSU. All fish collected in each sample were identified, measured (TL and FL) and given one of two tag types following established fish handling protocols in Grand Canyon, and were subsequently returned to the HSU where they were captured. We examined all appropriately sized fish for PIT tags, fin clips, FLOY (t-bar anchor) tags, and/or Visible Implant Elastomer (VIE) tags. Humpback chub, catfish, and carp greater than 100-mm TL, as well as brown trout and other natives greater than 150-mm TL received a PIT tag. Rainbow trout 200 mm TL and greater received a FLOY tag, and all other fish greater than 40 mm TL received a VIE tag that identified which gear and Site (1, 2, or 3) the fish was captured (the marks are not unique to individual fish). The use of VIE marks was required because the smaller size fish are too small to mark with PIT tags. We sampled each site over 3 nights and kept track of the cumulative numbers of captures and recaptures of fish (all species and tag types). We used this mark-recapture information to estimate abundance for each site.

Field efforts in 2011 included a total of four sampling trips, two trips prior to the planned steady flow experiment and two during the steady flow experiment. High precipitation during winter 2010-2011 created different mainstem flow conditions in July and August than in 2009-2010 with 2011 flows steady, but higher, than flow conditions observed in earlier sampling years (Figure 2). Two trips launched during these higher flow conditions (mid-July and mid-August 2011), and two trips launched following the start of the steady flow experiment (experiment began September 1, trip launch dates early September and mid-October; Figure 2 all years of flows). Colorado River turbidity was low for the July trip and most of the August trip with higher turbidity in September and October (Figures 3 - 5). Water temperatures during 2011 were warmer than in 2009 or 2010 and also one of the warmest in recent years, exceeding the mean 2003-2008 temperature by about 1 ºC and the 1994-2002 mean by about 4 ºC (Figure 6).

Sampling selectivity is thought to differ among gear type, and for a given fish species, body size, or habitat. In Sites 1 and 2, in addition to electrofishing, we deployed hoopnets (standardized mini-hoopnets used by cooperating agencies for

mainstem fish sampling, approximately 0.5-m in diameter, 1.0-m length, 6-mm mesh, and single 10-cm throat; n = 80 nets). Hoopnets were checked every 24-hours and were fished for 12 nights for each trip. All collected fish were processed similarly to the fish captured via electrofishing.

Water chemistry and isotope sampling

Water samples were collected in July, August, September, and October 2011. Acidified (1% HNO_3) samples were analyzed for trace elements with inductively coupled plasma optical emission spectrometry (ICP-OES) or inductively coupled plasma mass spectrometry (ICP-MS). Our limit of detection for most elements was in the low parts per billion. Following completion of quality control samples, results were only accepted if relative standard deviation (standard deviation / mean * 100) < 10%. Unacidified samples were analyzed for stable isotopic ratios of O, H, and C. Oxygen ($\delta^{18}O$) and hydrogen:deuterium (H:D) ratios were analyzed by isotope ratio mass spectrometry at the Center for Stable Isotope Biogeochemistry at the University of California at Berkeley. Carbon ($\delta^{13}C$) ratios were analyzed at the Stable Isotope Facility at the University of California at Davis. Strontium isotopes were not analyzed in 2011, because previous work indicated that these would not serve as good discriminators between the Little Colorado River and the mainstem.

Movement and growth assessment from otoliths

The use of otolith chemistry as a natural marker is based on a predictable relationship between water and otolith chemistry such that fish movements between water masses with differing trace elemental chemistry is reflected in otolith composition. As an example of our work so far, humpback chub (*n* = 10) were obtained from collections maintained by the USGS Grand Canyon Monitoring and Research Center in Flagstaff, Arizona for otolith chemistry investigations. In the Colorado River, fish were available from the 30-Mile Spring aggregation (~48 rkm), the Colorado River-Little Colorado River confluence aggregation (~100 rkm), and the final 12 km of the Little Colorado River aggregation (Table 3). We chose these aggregations to represent a range of possible provenance and life history trajectories. Of the ten fish included in this

study, eight individuals in the collection were small, presumed juveniles and two individuals were larger adults or subadults (Kaeding and Zimmerman, 1983).

Lapillar otoliths were selected for otolith chemistry analyses and were removed via dissection and cleaned of any adhering organic matter by immersion in a dilute (10% V:V) bleach-water solution. Preparation of otoliths for microchemical analyses was adapted from Secor (1991). A single otolith was randomly chosen for elemental analyses and was cast into rectangular molds using EpoFix (Struers) cold-set epoxy. Epoxy blocks were sectioned in the frontal plane through the core with a low-speed diamond saw (Buehler- IsoMet) and then polished using progressively finer grades of aluminum oxide lapping film until the otolith core was exposed, as determined by bright-field light microscopy. Polished otoliths were subsequently mounted on fused-quartz glass slides using cyanoacrylate adhesive (Loctite). Immediately prior to elemental analyses, all samples were ultrasonically cleaned in deionized water. Otoliths were photographed at magnifications of 200 – 630X and the daily rings were counted without prior knowledge of the identity of the fish. For the two larger fish, ages in years were determined, and daily rings deposited from hatch during the juvenile phase were enumerated until growth slowed so much that daily rings could no longer be discerned.

Multiple otolith trace elemental concentrations were quantified using scanning x-ray fluorescence microscopy (SXFM) at the F3 beamline station at the Cornell High Energy Synchrotron Source (CHESS). Scanning x-ray fluorescence microscopy is a spectral technique that uses high energy x-rays to produce an elemental fluorescence spectrum. A double-bounce multilayer monochromator provided a 16.1 keV incident beam with 0.6% bandpass. A single-bounce glass capillary was used to focus the incident beam to a 20-µm (horizontal) by 10-µm (vertical) spot at the sample with a photon flux of approximately 10^{11} counts per second (Bilderback *et al.*, 2003; Cornaby, 2008). Two-dimensional surface maps of elemental concentrations were created by stepping the beam across the entire surface of the sample in a sequential, non-overlapping grid pattern. At each step, the fluorescence spectrum was integrated for 1–3 seconds before moving to the adjacent sample location. Fluorescence x-rays were detected with a Vortex energy-dispersive silicon drift detector fitted with an aluminum foil attenuator to reduce high intensity calcium fluorescence and increase sensitivity to

trace elements. Initial spectral processing consisted of screening for a suite of 25 trace elements. Only Se, Sr, and Ca concentrations exhibited consistent variation between and within fish, but some other elements (e.g., Zn) were occasionally detected in meaningful patterns (i.e., were incorporated into the otolith structure and were not specimen contamination). Samples are reported as molar ratios to Ca (millimole element:mole Ca) (Campana, 1999). Instrumental calibration was achieved using an in-house standard reference material consisting of ground otolith material of known trace elemental concentrations (Limburg *et al.*, 2011). Data reduction and processing were completed using PyMCA (Solé *et al.*, 2007) and in-house software developed at CHESS to produce 2-dimensional elemental maps and spatially explicit numerical output. Numerical data were imported to a geographic information system to extract sequences (i.e., transects) of elemental concentrations from the two-dimensional maps (Quantum GIS Development Team, 2011). All elemental sequences extended from the otolith core to the otolith edge, parallel to the longest growth axis of the otolith.

In addition to analyses of trace elements in water and otoliths, in-situ carbon stable isotope measurements of one juvenile humpback chub otolith were conducted using the CAMECA IMS 1280 Secondary Ion Mass Spectrometer (SIMS) instrument at the Northeast National Ion Microprobe Facility (Woods Hole, MA). This instrument is a large radius, double focusing mass spectrometer fitted with an ion detection system consisting of two Faraday cups and a single electron multiplier. The secondary ion extraction system consisted of a Cs^+ ion beam combined with a high energy normal-incidence electron gun for charge compensation. Ions were extracted by rastering the beam over the surface of the sample in a 30µm x 30µm pattern. Estimates of $\delta^{13}C$ and the precision of the estimates were calculated by bracketing unknown otolith analyses with analysis of an in-house standard reference material (Carrara marble). Results are reported as per mille Pee Dee Belenite. The humpback chub otolith was analyzed at one location near the otolith core and again near the otolith edge. As with SXFM analyses, the humpback chub otolith was embedded in epoxy, cut in a frontal plane, and polished with progressively smaller diamond grit until the otolith core was exposed at the surface (final polish = 0.05 micron diamond suspension). The SIMS instrument sample holder accepts round 25.4-mm round samples and as such, the embedded

otolith with standard reference grains were pressed into a round (25.4 mm diameter) indium metal plug. In addition to providing a secure method for mounting the sample in the instrument, the indium disk also minimizes background interferences. Immediately prior to analysis, samples were ultrasonically cleaned in deionized water and sputter-coated with gold.

Results and Analyses to date

Catch and size frequency analyses

Across all four trips in 2011, in all sites, using both gears, we collected over 15,000 fish from 12 identifiable species (Table 1 and Table 2). The top three species caught (by number) were HBC (8295 caught), RBT (2653 caught), and bluehead sucker (1465 caught). We focus the remaining results in this report on 2011 field season results for juvenile HBC as they are the species of primary management interest in this system.

Size frequency analyses show that both gears (HN and EF) captured a wide size range of HBC (Figures 8 and 9). In 2011 there was not a large difference in the minimum size of fish collected by either gear, and both gears appeared to collect HBC < 100 equally well. Total catch of all sizes of HBC was higher with hoopnets than electrofishing (Figures 8 and 9). Hoopnets also caught more large HBC than electrofishing. A density plot for both gears combined and each trip in 2011 shows the highest density in size for HBC < 100 across all trips (Figure 10). This density plot also shows that the size distribution across trips was fairly similar and the progressive increase in the peak modal length each trip indicates growth (Figure 10).

Spatial distribution of catch, movement, and habitat use of HBC

To examine the spatial distribution of HBC catch, we created a table of tagging and recapture locations (Table 1) and a plot of HBC catch by size class on habitat sub-unit (HSU; Figure 11). The HSU represents the spatial grid cell of each electrofishing transect sample. We structured this plot such that the HSUs for river right (sites 140-300) are found on the primary x-axis and the HSUs for river left (HSU 450-650) are

found on the secondary x-axis (Figure 11). The catch in each of these grid cells (y-axis) then corresponds to each x-axis such that catches close to zero for a given HSU are near the axis corresponding to that HSU (either primary or secondary x-axis) and non-zero catches are a greater distance away from the corresponding x-axis. Catches of HBC of all sizes by gear and trip were widely distributed throughout each site for electrofishing and a similar pattern is apparent for HBC in hoopnet samples in Site 1.

Movement of tagged fish

Movement patterns of VIE tagged HBC are detailed in Table 1 which identifies total catch in each site on each trip, and then recaptures in all other possible trip and site combinations. As a reminder, VIE tagged HBC are < 100-mm TL. Movement patterns of HBC within a trip were generally restricted to the site of tagging with the majority of recaptures occurring in the same site in which the fish was tagged. Recaptures of fish outside of the site they were originally tagged occurred both downstream and upstream (i.e., Trip 3, Site 2, 1 fish was recaptured in Site 1; Table 1). Highest marking rates were in Site 1 and Site 2 because of the additional sampling effort associated with fishing hoopnets in these sites. We also cooperated with USFWS to VIE mark HBC < 100-mm TL in the LCR with a trip specific VIE mark. In this way we hoped to identify the timing of outmigration from the LCR to the mainstem through recaptures of LCR origin VIE marks during our mainstem sampling. Juvenile HBC were marked in the LCR during July and August through limited sampling (10 nets) and in September and October by the USFWS as part of their standard fall monitoring programs. Despite marking over 1154 fish with VIE in the LCR in 2011(844 by FWS and 310 by NSE), only 5 were collected during NSE mainstem sampling. Alternatively 3 fish VIE marked in the mainstem by NSE personnel (all from 2009 sampling) were recaptured in the LCR in 2011.

Capture probability

We assessed capture probability of juvenile HBC in two different size classes, for fish < 100-mm TL we used recaptures of VIE marked fish and for HBC 100-200-mm TL we used PIT tag recaptures. As expected, capture probabilities were low for both sizes

of HBC. We also have persistently noted a difference in the capture probability of unmarked fish (first captures capture probability = 5-15%) and subsequent recaptures (recapture probability = 3-8%. These differences are not uncommon in mark-recapture studies and likely reflect a short-term response to fish being captured or recaptured. It is likely that fish are either using slightly different habitats following their initial capture (such as moving deeper following capture, marking, and release) or simply choose not to use a hoopnet as cover. We also observed a decline in capture probability across sampling passes which is also likely related to the behavioral responses to handling. This decline over subsequent passes is likely a function of our samples first capturing and marking fish that either use habitats that are highly vulnerable to our gear, and, after marking all of those "easier to capture" fish our capture probabilities decline as the remaining individuals to be captured are in habitats where it is more difficult to collect them (Figure 12; decline in p-hat by pass). We are currently working to incorporate turbidity, flow, and other physical factors as covariates on capture probability.

Abundance

We are currently assessing a variety of approaches to estimating abundance to find an approach that is robust to the low and variable capture probabilities observed. Our approaches include a variety of standard closed population estimators covered in Williams et al. (2002) as well as original models we are developing that will integrate information from all NSE sampling trips to develop a better understanding of the probably distribution of capture and recapture probabilities. This integration will come from sharing information on capture and recapture probability between gears and sites as well as across years. This approach will be completed in a hierarchical approach which should allow for better assessment of covariates such as fish size or turbidity thought to influence juvenile HBC catch. This integrated approach is being developed closely with GCMRC cooperators.

A major difficulty we have encountered in more rapidly developing a robust model for abundance has been the difficulty in efficiently compiling summary data of marks and recaptures. This is particularly true for the VIE marked fish as these fish can

accumulate multiple VIE marks as they are captured (and recaptured) on different trips or gears or sites. This has required tedious reconstructions of the individual capture histories for these fish. Working with GCMRC staff we have recently made major advances in automating this process. For purposes of this report, as in 2009, we estimated abundance of juvenile HBC using closed population models described by Gazey and Staley (1986). Abundance of HBC < 100-mm TL maximum likelihood estimates (MLEs) and uncertainty profiles for each site and trip (Figures 13-17) show that abundance in Sites 1 and 2 were fairly similar (approximately 700 -1500 fish). Estimates for Site 3 were slightly lower with MLE estimates < 500 fish. Estimates with very high uncertainty (i.e. Trip 1, Site 1 electrofishing or Trip 2, Site 3 electrofishing; Figure 13) where convergence was not met and estimates are not possible was likely due to extremely low (if any) recaptures of marked fish. We developed estimates for each gear type separately in Site 1 and Site 2 (hoopnets blue line, electrofishing black line) and found generally similar patterns and overlapping likelihood profiles with each gear type (Figure 14). Abundance in Site 1 appears to have increased throughout 2011 likely related to emigration of juvenile HBC from the LCR to the mainstem. These same increasing abundance patterns are not apparent in the other sample sites. We also assessed how many samples were necessary to generate parameter estimates for each gear type (Figures 15 and 16). Figure 15 provides an example of this type of inference where we have plotted the abundance estimates for HBC in Site 1 for Trip 1 from electrofishing after each nightly pass. Each line on the graph represents an abundance estimate following a night of sampling where the flat line represents the abundance estimate after sampling 1 night (no estimate, as no recaptures were made) and then the subsequent night (night 2) of sampling all yields a poorly defined likelihood estimate (not a well defined dome). After the third night of sampling the estimate is much better defined and the MLE estimate (thick black line) of abundance is plotted. Figure 16 shows the same type of graph for hoopnetting where generally sigmoidal (logistic) curves are plotted for each night of sampling, until sufficient recaptures are made (after approximately seven nights of sampling) resulting in a defined likelihood estimate (dome shaped curve) that with subsequent samples (and recaptures) becomes better defined (until MLE is reached, thick black line). These plots demonstrate that at least three

nights of sampling are needed to generate estimates of abundance using electrofishing and seven nights of sampling are needed for hoopnetting (Figure 17).

A second difficulty we have encountered is in the accounting for tracking the mark and recapture information for VIE marked fish as they grow and transition to PIT tagged fish. The VIE marks are not unique (batch mark indicating trip, gear, and site) but the PIT tags are a unique mark. We are still working on an efficient way to track these capture histories for fish that have transitioned from VIE to PIT tags. For now, we are estimating abundance of fish 100-200 mm TL using only PIT tag data. For this report we estimated abundance of HBC between 100-200 mm TL for each trip of the NSE project using a closed population model in program MARK. Abundance estimates from this model for HBC 100-200 mm TL across all 12 NSE trips (2009-2011) are generally about 1500 fish and range from about 1000-2000 HBC (Figure 13).

In this model we allowed capture probability to vary by trip and we set recapture probability equal to capture probability. The data were pooled in this way, even though we suspect that recapture probabilities are lower than capture probability estimates, because in some trips capture or recapture probability estimates were un-estimable because of sparse recaptures. When capture probability = recapture probability this shared term is estimable. The result of setting these two parameters equal likely causes negative bias in the shared capture probability-recapture probability estimated for each trip (capture probability generally 1-2%) resulting in a positive bias of abundance. During 2012 we will explore this bias and develop an approach which describes a distribution of capture and recapture probabilities from which to draw from to estimate abundance in the recapture sparse sampling events or pools across habitat types (Figure 18).

Apparent Survival

To calculate juvenile humpback chub apparent survival rates using the Cormack-Jolly Seber recaptures-only model (Lebreton *et al.* 1992), fish must be able to be individually tracked over time. Although VIE (batch) marks make this difficult (you can't distinguish between *individual* fish, although you can decipher a capture history), we were able to create capture histories for all fish large enough to be tagged. We

estimated annual apparent survival rates for humpback chub that were VIE tagged upon first capture (TL <100 mm). Some of these fish grow into PIT tag sizes, but these individuals were still included in juvenile humpback chub apparent survival analyses, as even the fastest growing individuals still remained juveniles (<200 mm TL) over the duration of the NSE study.

The highest ranking model of our analyses estimated juvenile humpback chub apparent survival by year (close ranking models estimate survival by flow). Results indicate that apparent survival point estimates in 2011 are lower than in either 2010 or 2009 (~20% versus ~50% and ~70%, respectively; Figure 19), but the confidence intervals overlap to a high degree. The "trumpet" shape in precision of apparent survival estimates through time (Figure 19) is common to capture recapture experiments due to limited recapture opportunities for fish handled in 2011. Additional monitoring in 2012 and beyond will be crucially important in refining these estimates, and we expect 2012 survival estimates to improve both in empirical value and in precision as data from the Natal Origins project becomes available. This monitoring will also be crucial in distinguishing between temporal effects on apparent survival and flow effects on apparent survival, as currently these models are distinguished by fewer than 5 ΔAICc points, making them statistically identical.

Growth

We estimated growth of juvenile HBC by counting daily growth increments on otoliths and through recaptures of PIT tagged fish. Otolith age estimates were made from HBC provided by cooperators or as incidental mortalities on this project over multiple years and sizes of fish. Because PIT tags provide unique marks, when we recapture a fish we can review the previous capture information to determine how much the fish has grown over the period of time since its last capture.

Growth from otolith samples

We compared growth of fish < 1 year of age from both the LCR (15-94 mm TL) and mainstem (18-139 mm TL) Colorado River. The majority of these fish were incidental mortalities from cooperators or the NSE project. The LCR young-of-year

(YOY) fish ranged from 15-94 mm TL and these fish were generally < 50 days of age, but several individuals were determined to be over 120 days old. A linear model of age-length estimated daily growth as about 0.49 mm/day (TL = 0.4859x + 7.2357 R^2 = 0.9149). Young-of-year chub from the mainstem were a much wider range of sizes from 18–139 mm and the range of age for a given size was much wider than in the LCR. A linear model was not as good a fit with the mainstem growth data (R^2 = 0.5004) and estimated daily growth rate was the same (0.48 mm/day, TL = 0.4883x + 0.889) as the LCR. We combined our age-1+ fish from the LCR (n = 17) and mainstem (n = 19) for growth analyses as these age fish are known to mix between the two rivers. We fit a standard von Bertalanffy growth curve to these data (L_{inf} = 412, k = 0.09, t_o = -1.74; Figure 20).

Growth from PIT tag recaptures

We assessed growth of juvenile HBC in both the mainstem Colorado River and the LCR for summer (July-August, Figure 21) and fall (September-October, Figure 22) periods over the entire NSE project duration (2009-2011, Figure 23). Fish were included in our analyses if they were <200 mm TL when they were first captured (juveniles), and were subsequently recaptured the very next trip. We had to exclude fish that were recaptured over longer time intervals both because of closure assumptions and because the growth rates could not be readily assigned to specific flow treatments. Because of small sample sizes associated with recaptures of fish available from growth assessment, we bootstrapped our estimates of growth 1000-times to create frequency distributions of growth under each location and time interval.

2011 growth rates in the mainstem Colorado River were higher during the fall steady flow period compared to the summer steady flow period (Figures 21 and 22), in contrast to 2009 and 2010 when growth of juvenile HBC from the mainstem Colorado was slower in September and October (steady flows) than in July and August (fluctuating flow, Figures 21 and 22). Water temperatures were similar across both time periods within each year (Figure 6). LCR growth was generally faster (but highly variable) in July and August than in September-October (Figures 23 and 24) although higher daily growth rates in 2010 seemed to be sustained into the fall.

The invaluable (albeit serendipitous) high water year of 2011 provided an important contrast in growth rates during various flow regimes. Previous results on daily growth rates of juvenile humpback chub during steady flows were confounded with potential seasonal declines in growth. 2011, however, provided us with a crucial summer steady flow experiment, although at a higher magnitude than previous summer fluctuating flows (Figure 2). The fall period of 2011 then demonstrated higher growth rates in the mainstem COR (Figure 22). This data indicates that, even during the same season, growth rates during steady flows are lower than corresponding growth rates during fluctuating flows. Other factors such as magnitude of flow and fish density may be influencing these growth rates as well as or even instead of flow variability. We acknowledge openly that replicates are needed to give additional scientific credence to the conclusion of lower growth during steady flows. However, a cessation of summer and/or fall steady flow experiments coupled with a reduction in NSE-style monitoring precludes the possibility of refining these conclusions.

Growth assessment via changes in length-weight relationship

We examine the relationship between juvenile humpback chub length and weight in both Colorado River and Little Colorado River to examine whether differences exist spatially (mainstem vs. LCR) as well as whether the length-weight relationship changed seasonally within a year and system. We fit the standard model of fish weight to length $W=aL^b$ where W is fish weight in grams, L is fish length in mm and a and b are model parameters to data collected in the mainstem Colorado River or in the Little Colorado. We estimated model parameters using a non-linear optimization routine (Microsoft SOLVER). We interpreted model parameters as outlined in Froese (2006) where b is the exponent of the arithmetic relationship and that b represents the "direction and rate of change of form or condition" for a fish (as in Hile (1936) where $b < 3.0$ indicates a decline in the condition or elongation in fish form with an increase in length and a $b > 3.0$ indicates an increase in condition, height, or width with an increase in length. The a parameter is simply interpreted as a scaling coefficient. We restricted our analyses to (1) fish less than 200-mm TL which are likely juveniles to eliminate any changes in length and weight related to reproduction, (2) samples collected only during

the late summer or early fall monsoon season to eliminate seasonal variation in growth or condition, (3) samples with similar gear types to reduce gear bias. In 2011 weight and length data were collected for 633, 835, and 478 humpback chub in the mainstem during August-October that met these criteria and 100 humpback chub in the LCR met the criteria in August. We developed a test of coincident curves as a likelihood ratio test (Kimura 1980; Haddon 2001) to test for differences in the relationship between weight and length under the following scenarios: (1) we tested for differences between months within the mainstem to see if the *b* term changed through time and (2) we compared the LCR and mainstem for 2011.

In the mainstem Colorado River, the test for coincident curves yielded significant differences between curves ($p < 0.001$). Both the *a* and *b* parameters were found to be significant ($p < 0.001$) for all months (Figure 25). The month of August had the highest *b* parameter of 3.21 and declined to 3.11 then 3.02 during September and October. We mined archival data that met our guidelines for both the mainstem and LCR and were able to obtain 5 years of data where length and weight data were simultaneously collected in the mainstem and LCR. Graphical comparison of length-weight relationship for juvenile fish from these years shows that the *b* term is trending lower in the mainstem and *b* is increasing in the Little Colorado River (Figure 26).

Water Chemistry

Spatial trends in water chemistries

Water chemistry of the Colorado River and tributaries in Grand Canyon was spatially and temporally heterogeneous for Sr:Ca, Se:Ca, DOC $\delta^{13}C$, and DIC $\delta^{13}C$ across sites and sample dates. Compared to the Colorado, tributary water chemistry exhibited substantially more variability. Water chemistry of the Colorado River was similar throughout the entire Grand Canyon and this consistency of water chemistry throughout the Grand Canyon suggests that tributary inputs to the Colorado River are small and quickly diluted. Furthermore, Lake Powell is a large reservoir and serves to homogenize the water chemistry at the beginning of the Grand Canyon reach of the Colorado River. With the possible exception of Paria River and Nankoweap Creek, all tributary multivariate water chemistry signatures are likely readily distinguished from the

mainstem Colorado River. Comparing tributary water chemistry, Bright Angel, Tapeats, and Shinumo creeks were similar but had lower trace element and isotopic elemental ratios compared to the Colorado River (Figure 7). The Little Colorado River, Havasu Creek, and 30-Mile Spring had water chemistry characterized by high $\delta^{13}C$ values and low element to calcium ratios compared to the Colorado River chemistry (Figure 7).

Provenance, movement and growth from otoliths

We summarized the age and growth of fish collected in the mainstem and LCR and provided to us by cooperators for age analysis from multiple years of sampling (Figure 27). These age-growth relationships will continue to be updated as additional data become available. Ten fish were analyzed in depth (paired age and growth assessment and microchemistry) and are reported on here. The following information is based upon a manuscript in review in *River Research and Applications*.

The age and growth history of Fish-1 (Table 3) corresponded well to otolith chemistry. From hatching, there were 37 large, distinct daily growth increments, followed by 59 very small increments, followed by a period of such slow growth that we could only estimate the number of growth rings as 40-45. This last period corresponds to the increase in Se:Ca and Sr:Ca and decline in $\delta^{13}C$, confirming that summer time growth rate slows.

Fish-2 exhibited a complicated migration history based on otolith Sr:Ca ratios. The otolith Sr:Ca transect of Fish-2 was similar to Fish-1, suggesting that this fish originated in the Little Colorado River and migrated to the Colorado River. However, this individual (Fish-2) was collected in the LCR approximately ~1.1 km above the Little Colorado-Colorado river confluence, despite the Colorado River Sr:Ca ratio at the otolith edge. The mismatch between collection location and edge otolith chemistry may be explained by recent immigration to the LCR such that its otolith chemistry had not equilibrated with the water at the collection location. This fish had over 140 visible daily growth increments, and apparently overwintered in the Colorado mainstem, and thus should be classified as a 1+ year old fish rather than a juvenile. We note its very small size (37-mm) (Table 3).

Three juvenile humpback chub were available that were collected in the Colorado River upstream of the LCR. Two of these fish (Fish-3 and Fish-4) had core Sr:Ca chemistry that was similar to the resident Little Colorado River specimens (Fishes-6, 7, and 8) but also had increasing Sr:Ca ratios between the otolith core and edge, similar to Fish-1 that migrated from the Little Colorado River to the Colorado River. Taken at face value, this suggests that Fish-3 and Fish-4 originated in the Little Colorado River and moved to the Colorado River. However, Fishes-3 and -4 were collected in the Colorado River at rkm 64.6 (~ 38 km upstream of the LCR – Colorado River confluence) and were very small (19 and 18 mm TL, respectively; Table 3). Although it cannot be ruled out, it is unlikely that Fish-3 and Fish-4 originated in the Little Colorado River swam against the current 35 km upstream to the collection location as ~20 mm-TL individuals. The 30-Mile Spring region (rkm ~48) of the Colorado River contains a number of warm springs associated with Fence Fault in which larval humpback chubs have been observed and thought to have been spawned (Valdez and Masslich 1999; Andersen *et al.*, 2010). Mantle-derived groundwater feeds both the 30-Mile Spring complex and the Blue Spring in the Little Colorado River and as such, water chemistry of 30-Mile Spring is similar to the Blue Spring and both spring complexes are outlets for warm water with high carbon-dioxide loads (Crossey et al. 2006; Crossey et al. 2009). Although our analyses of Little Colorado River and 30-Mile Spring water chemistry suggest that fish residing in these locations should result in unique otolith chemistry signatures, we sampled only one spring in the area. It is possible that an unknown spring (possibly subaqueous within the Colorado River) in the area may have indistinguishable water chemistry from the Little Colorado River and support limited humpback chub spawning. Additional analyses of fish and water samples collected from 30-Mile Spring are needed to differentiate these locations with confidence. Therefore, it is plausible that Fish-3 and Fish-4 may have originated in the 30-Mile Spring area and subsequently drifted downstream prior to capture.

Furthermore, Fish-3 and Fish-4 were collected as ca. 20-mm individuals in September 2006. Such small sizes in the Little Colorado would correspond to fish around a month in age; however, Fish-3 had 83 daily growth increments (Figure 28, lower panel; Fish-4 was slightly over-polished and could not be aged). Fish-3 was

therefore hatched in mid-June 2006, later than the primary humpback chub spawning period of March – May. As well, Fish-3 had approximately 2 weeks of initially high growth, followed by a rapid transition to very slow, even growth (Figure 28). Thus, we interpret Fish-3 (and Fish-4) as having reared in a nursery area in the 30-Mile Spring complex, after which they were advected into the mainstem and survived, albeit with very slow rates of growth.

Although the otolith core Sr:Ca chemistry and capture location of Fish-3 and Fish-4 suggest a complex migration trajectory, the edge chemistry of these otoliths was similar to the edge chemistry of Fish-1, suggesting that these individuals spent sufficient time in the Colorado River to obtain a Colorado River otolith signature where they were collected. Again, this corresponds well with the growth history (Figure 29). The otolith chemistry of Fish-5, collected in the Colorado River upstream of the LCR, had an unique Sr:Ca chemistry compared to all other fish in this study. As with Fish-3 and Fish-4, this individual was collected downstream (rkm ~78) of the 30-Mile Spring as a 21-mm TL individual in September 2006 and was aged to 75 days (Table 3). The Sr:Ca transect between the otolith core and edge of this fish was characterized by a constant, low Sr:Ca ratio. In fact, the constant chemistry between the otolith core and edge and the fact that its chemistry was lower than any other fish in the study suggests that this fish was not spawned in the LCR. The low otolith chemistry of this fish does not match the typical mainstem Colorado River chemistry signature which all other fish analyzed to date have incorporated into their otoliths. As such, given our knowledge of water chemistry in the system this fish likely spawned in a previously unknown site within the Colorado River and exhibited high site fidelity to this location. However, Fish-5's daily growth increments were very narrow, suggesting cooler water conditions in the unknown nursery habitat than in the Little Colorado or 30-Mile Spring nurseries.

Fish-9 and Fish-10 (Table 3) were larger humpback chub and their otolith chemistry transects exhibited multiple Sr:Ca and Se:Ca peaks between the otolith core and edge. In both fish, the maximum Sr:Ca ratio observed in the transect was located approximately 40 - 60% of the distance between the core and edge with subsequent Sr:Ca peaks decreasing towards the otolith edge. Although the maximum Sr:Ca ratios in Fish-9 and Fish-10 are higher than observed in Fishes-1-8, this may represent inter-

annual variation in site-specific otolith chemistry owing to basin-wide processes such as Glen Canyon Dam releases or discharge within the LCR. Temporal shifts in otolith chemistry are well documented when comparing site-specific otolith chemistry across multiple years (Gillanders 2002). Given our observations of high Sr:Ca ratios with Colorado River residency and low Sr:Ca with Little Colorado River residency, the multiple peaks in the adult humpback chub chemistry between otolith core and edge is likely representing multiple fish movements between the Little Colorado and Colorado rivers.

Otolith Se:Ca ratios also increased between otolith core and edge in the adult humpback chub. In the largest adult fish included in the study, (Fish-10, TL = 255 mm) Se:Ca peaks were positively correlated with Sr:Ca, as expected by water chemistry analyses. In Fish-9, the correlation between otolith Sr:Ca and Se:Ca was observed but not as strong. Fish-9 was a 1+ and Fish-10 a 5+ year old fish (Figure 29). Otolith daily increments deposited during the first growing season were visible out to 138 days and 176 days, respectively. We note the stark contrast between Fish-9 (112 mm) and Fish-2, originally thought to be a 37-mm juvenile but with over 140 visible daily increments and a capture date of May, this is likely either a 1+ fish spawned in the spring or a fall spawned fish. Further analysis will reveal whether or not such small fish actually recruit to the adult population. We hypothesize that these fish are non-viable as recruits.

2012 Work plan

Our 2012 efforts are focused on finalizing analyses approaches and writing peer-reviewed manuscripts. These efforts will be developed in cooperation with all project participants, governmental agencies, Native American tribal and governmental organizations, and other research cooperators in Grand Canyon. We plan on making multiple trips to meet with these cooperators throughout 2012 to keep everyone up-to-date on progress and communicate findings of our work.

Acknowledgements

We are very appreciative of the excellent technical and logistical support services provided by USGS-GCMRC and Humphrey Summit Support. We are particularly appreciative to our boatmen for their expert assistance. We also thank AZGF for their tremendous logistical assistance throughout the project. USFWS, NPS, BOR, WAPA, Navajo Nation Department of Fish and Wildlife and others provided technical, permitting, logistical, and financial support for the entire project, thank you. We also acknowledge the University of Florida for providing partial financial support for graduate education as well as extensive contracting, salary support, and administrative assistance.

References

Andersen ME, Ackerman MW, Hilwig KD, Fuller EA, and Alley PD. 2010. Evidence of Young Humpback Chub Overwintering in the Mainstem Colorado River, Marble Canyon, Arizona, USA. *The Open Fish Science Journal* **3**: 42-50.

Bilderback DH, Huang R., Kazimirov A, Kriksunov IA, Limburg KE, Fontes E. 2003. Monocapillary Optics Developments and Applications. *Advances in X-Ray Analysis* **46**: 320–325.

Campana SE. 1999. Chemistry and Composition of Fish Otoliths: Pathways, Mechanisms, and Applications. *Marine Ecology Progress Series* **188**: 263-297.

Cornaby SW. 2008. The Handbook of X-ray Single Bounce Monocapillary Optics, Including Optical Design and Synchrotron Applications. PhD Dissertation, Cornell University: Ithaca, NY.

Crossey LJ, Fischer TP, Patchett PJ, Karlstrom KE, Hilton DR, Newell DL, Huntoon P, Reynolds AC, de Leeuw GAM. 2006. Dissected Hydrologic System at the Grand Canyon: Interaction Between Deeply Derived Fluids and Plateau Aquifer Eaters in Modern Springs and Travertine. *Geology* **34**: 25-28.

Crossey LJ, Karlstrom KE, Springer AE, Newell DL, Hilton DR, Fischer TP. 2009. Degassing of Mantle-Derived CO_2 and He from Springs in the Southern Colorado Plateau Region--Neotectonic Connections and Implications for Groundwater Systems. *Geological Society of America Bulletin* **121**: 1034-1053.

Gazey, W.J. and M.J. Staley. 1986. Estimation from Mark-Recapture Experiments using a Sequential Bays Algorithm. *Ecology* **67**: 941-951.

Gillanders BM. 2002. Temporal and Spatial Variability in Elemental Composition of Otoliths: Implications for Determining Stock Identity and Connectivity of Populations. *Canadian Journal of Fisheries and Aquatic Sciences* **59**: 669-679.

Kaeding LR, Zimmerman MA. 1983. Life History and Ecology of the Humpback Chub in the Little Colorado and Colorado Rivers of the Grand Canyon. *Transactions of the American Fisheries Society* **112**: 577-594.

Lebreton, J. D., K. P. Burnham, J. Clobert, and D. R. Anderson. 1992. Modeling Survival and Testing Biological Hypotheses Using Marked Animals: a Unified Approach with Case Studies. Ecological Monographs **62**: 67-118.

Limburg KE, Olson C, Walther Y, Dale D, Slomp CP, Hoie H. 2011. Tracking Baltic Hypoxia and Cod Migration Over Millennia with Natural Tags. *Proceedings of the National Academy of Sciences*. DOI: 10.1073/pnas.1100684108.

Solé VA, Papillon E, Cotte M, Walter P, Susini J. 2007. A Multiplatform Code for the Analysis of Energy-Dispersive X-ray Fluorescence Spectra. *Spectrochimica Acta Part B: Atomic Spectroscopy* **62**: 63-68.

Valdez, R.A. and W.J Masslich. 1999. Evidence of Reproduction by Humpback Chub in a Warm Spring of the Colorado River in Grand Canyon, Arizona. *The Southwestern Naturalist* **44**: 384-387.

Williams B.K., J.D. Nichols, and M.J. Conroy. 2002. Analysis and Management of Animal Populations: Modeling, Estimation, and Decision Making. SanDiego: Academic Press.

Table 1. Marks and recaptures of VIE marked humpback chub (<100-mm TL) across all trips and sites during 2011 NSE sampling. How to read this table: The trip column designates each of the 4 NSE trips in 2011 (July-October). Within each trip, fish are marked and released at a designated site (Sites 1-3). The M column represents the number of juvenile HBC VIE marked on each trip and site (< 100-mm TL). Each "Recaptures" column represents the number of fish recaptured on a given trip, at a given site (identified in the top row). As an example, 138 HBC were marked in July in Site 1, and 12 of these fish were recaptured that same trip; 11 in Site 1 and 1 in Site 2. 29 total fish from the 138 marked in July Site 1 were recaptured in August (25 in Site 1 and 4 in Site 2), etc..

							VIE Recaptures HBC < 100-mm TL						
	Marks	July Site 1	July Site 2	July Site 3	August Site 1	August Site 2	August Site 3	Sept Site 1	Sept Site 2	Sept Site 3	Oct Site 1	Oct Site 2	Oct Site 3
July Site 1	138	11	1	0	25	4	0	21	2	0	4	1	0
July Site 2	48	0	4	0	1	1	1	0	4	0	3	5	0
July Site 3	16	0	0	1	0	0	0	0	0	0	0	0	0
August Site 1	441				47	2	1	72	4	1	25	1	1
August Site 2	141				0	17	0	0	17	1	2	8	0
August Site 3	52				0	0	0	0	0	2	0	0	0
Sept Site 1	693							86	3	0	61	2	0
Sept Site 2	264							1	23	2	0	28	4
Sept Site 3	87							0	0	3	0	0	4
Oct Site 1	399										37	1	0
Oct Site 2	157										0	20	1
Oct Site 3	65										0	0	2

Table 2. Catch of all fish species from each site and trip during the 2011 field season using hoopnets and electrofishing. The percentages in the parentheses are the percent of the total catch for that site and trip composed of that species. Species abbreviations are defined in the list of abbreviations at the beginning of this report.

Combined Catch & Percent Table												
	GC20110709			**GC20110804**			**GC20110901**			**GC20111006**		
	Site			**Site**			**Site**			**Site**		
Species	**1**	**2**	**3**	**1**	**2**	**3**	**1**	**2**	**3**	**1**	**2**	**3**
BBH	1(0)	4(0.01)	7(0)	1(0)	1(0)	3(0)	5(0)	0(0)	5(0)	0(0)	0(0)	0(0)
BHS	66(0.08)	42(0.1)	155(0.1)	122(0.09)	126(0.17)	431(0.15)	115(0.07)	61(0.09)	205(0.07)	88(0.07)	31(0.05)	23(0.05)
BNT	2(0)	2(0)	5(0)	0(0)	0(0)	0(0)	1(0)	1(0)	2(0)	1(0)	1(0)	0(0)
CRP	9(0.01)	6(0.01)	20(0.01)	6(0)	5(0.01)	19(0.01)	2(0)	1(0)	7(0)	2(0)	0(0)	1(0)
FHM	18(0.02)	42(0.1)	150(0.1)	23(0.02)	71(0.1)	248(0.09)	57(0.03)	90(0.13)	366(0.12)	88(0.07)	132(0.22)	178(0.4)
FMS	55(0.07)	32(0.07)	102(0.07)	64(0.04)	23(0.03)	110(0.04)	78(0.04)	46(0.07)	152(0.05)	93(0.07)	45(0.08)	28(0.06)
GSF	0(0)	0(0)	0(0)	0(0)	0(0)	0(0)	0(0)	0(0)	0(0)	0(0)	1(0)	1(0)
HBC	387(0.49)	122(0.28)	546(0.35)	1011(0.71)	333(0.46)	1433(0.51)	1260(0.73)	373(0.53)	1734(0.59	797(0.61)	224(0.37)	75(0.17)
PKF	0(0)	0(0)	0(0)	3(0)	1(0)	5(0)	2(0)	4(0.01)	25(0.01)	5(0)	6(0.01)	11(0.02)
RBT	197(0.25)	153(0.35)	455(0.29)	153(0.11)	155(0.21)	484(0.17)	153(0.09)	107(0.15)	354(0.12)	189(0.15)	143(0.24)	110(0.25)
RSH	1(0)	0(0)	2(0)	5(0)	0(0)	6(0)	2(0)	1(0)	6(0)	2(0)	2(0)	1(0)
SPD	61(0.08)	33(0.08)	107(0.07)	36(0.03)	15(0.02)	79(0.03)	59(0.03)	20(0.03)	96(0.03)	31(0.02)	13(0.02)	20(0.04)

Table 3. Humpback chub biological data from otolith samples presented in this report. COR = Colorado River, LCR = Little Colorado River, Rkm = River kilometer (for COR, downstream of Lee's Ferry, AZ, for LCR = upstream of LCR, COR confluence), TL= total length (mm)

Fish	Collection Date	Collection Location	Rkm	TL (mm)	Age
1	20-Aug 2009	COR	101	33	140 d
2	May-2003	LCR	1.1	37	1+ yr
3	24-Sep 2006	COR	64.6	19	83 d
4	24-Sep 2006	COR	64.6	18	n.a.
5	25-Sep 2006	COR	78.1	21	75
6	Jun-2010	LCR	1.6	27	33 d
7	Jun-2010	LCR	3	28	39 d
8	Jun-2010	LCR	12	25	40 d
9	20-Jul 2009	LCR	1.6	112	1+ yr
10	7-Oct 2009	LCR	9	255	5+ yr

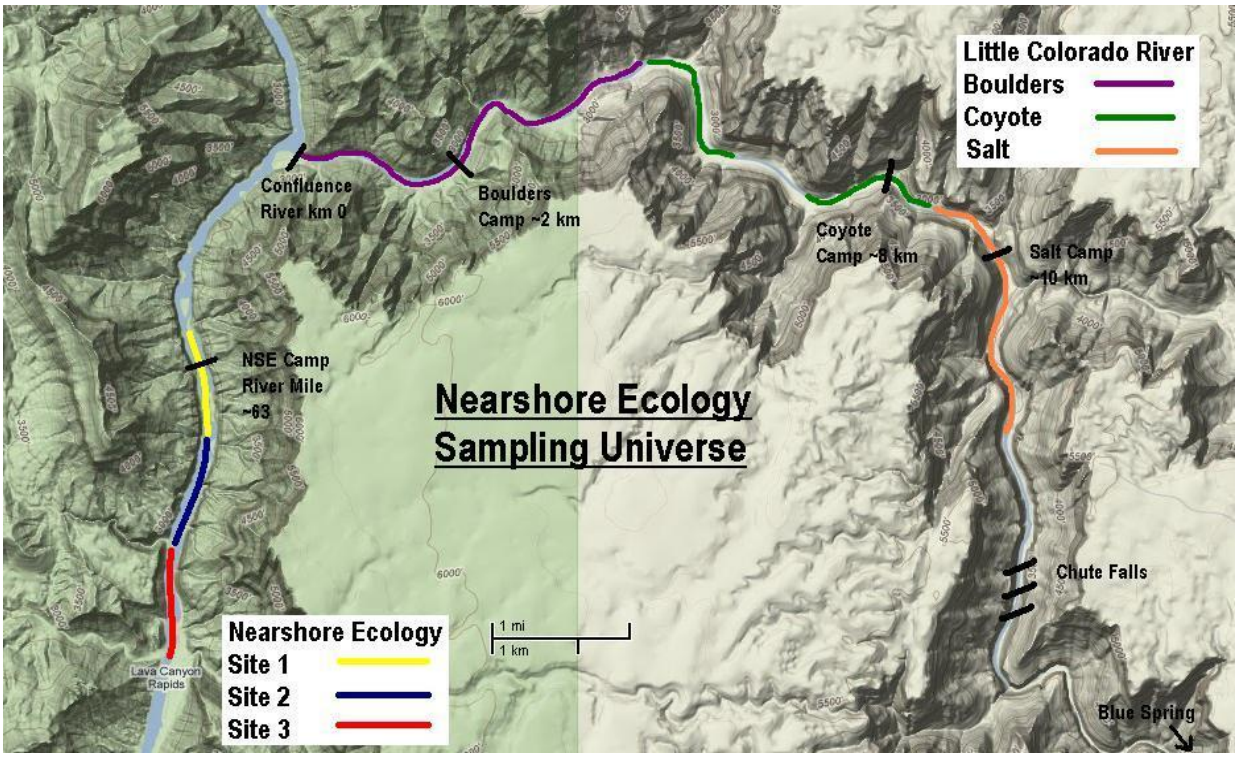

Figure 1. Map of the NSE sampling universe in the mainstem Colorado River, as well as the USFWS sampling base camps in the Little Colorado River.

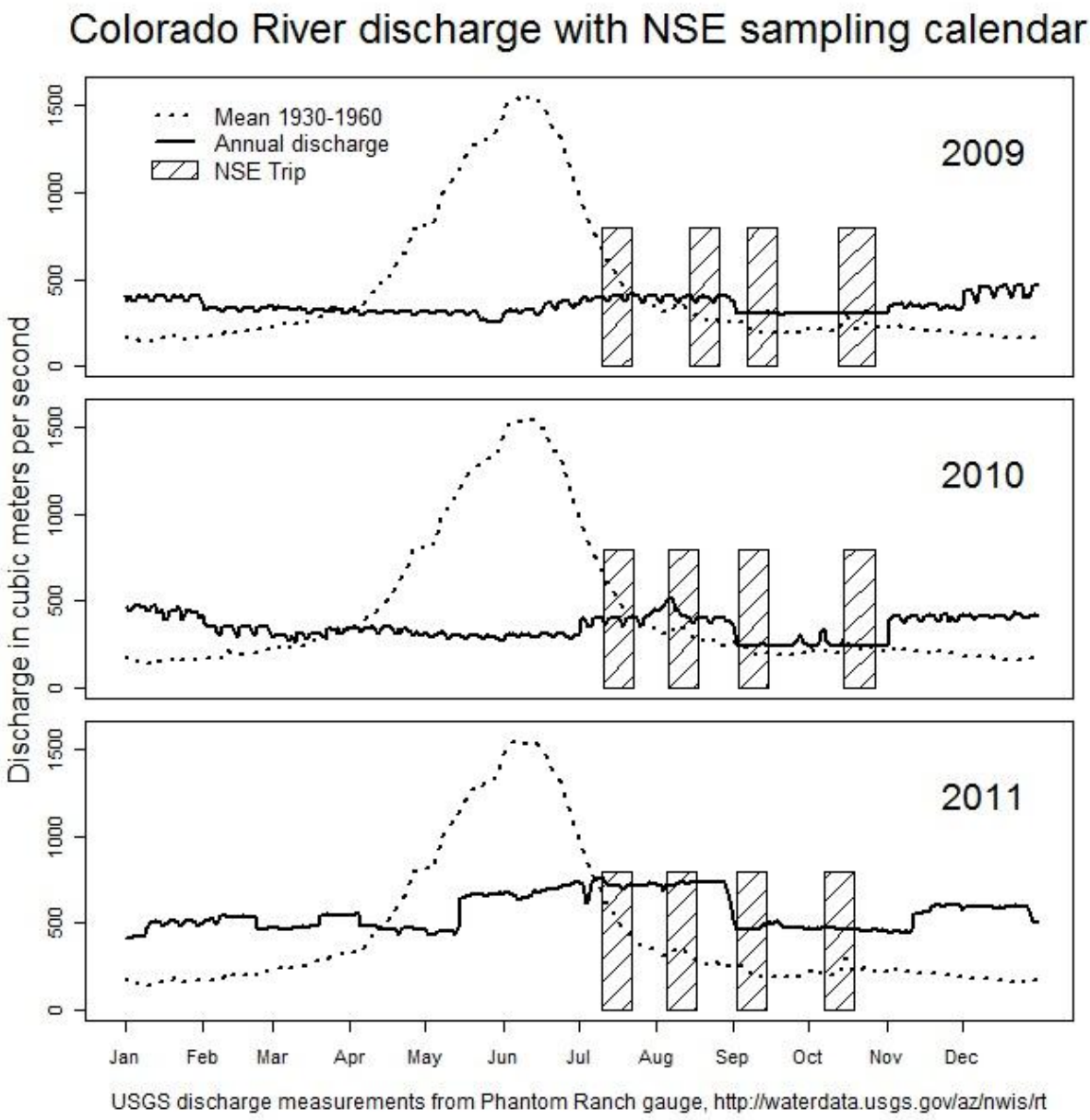

Figure 2. Discharge (m^3/sec) measurements from the Phantom Ranch gauge, as solid black lines, for the Colorado River during 2009 (top panel), 2010 (middle panel), and 2011(bottom panel). The dashed black line represents the mean discharge from 1930-1960, a time period which predates the completion of Glen Canyon Dam. The vertical striped rectangles represent the NSE sampling periods during each year.

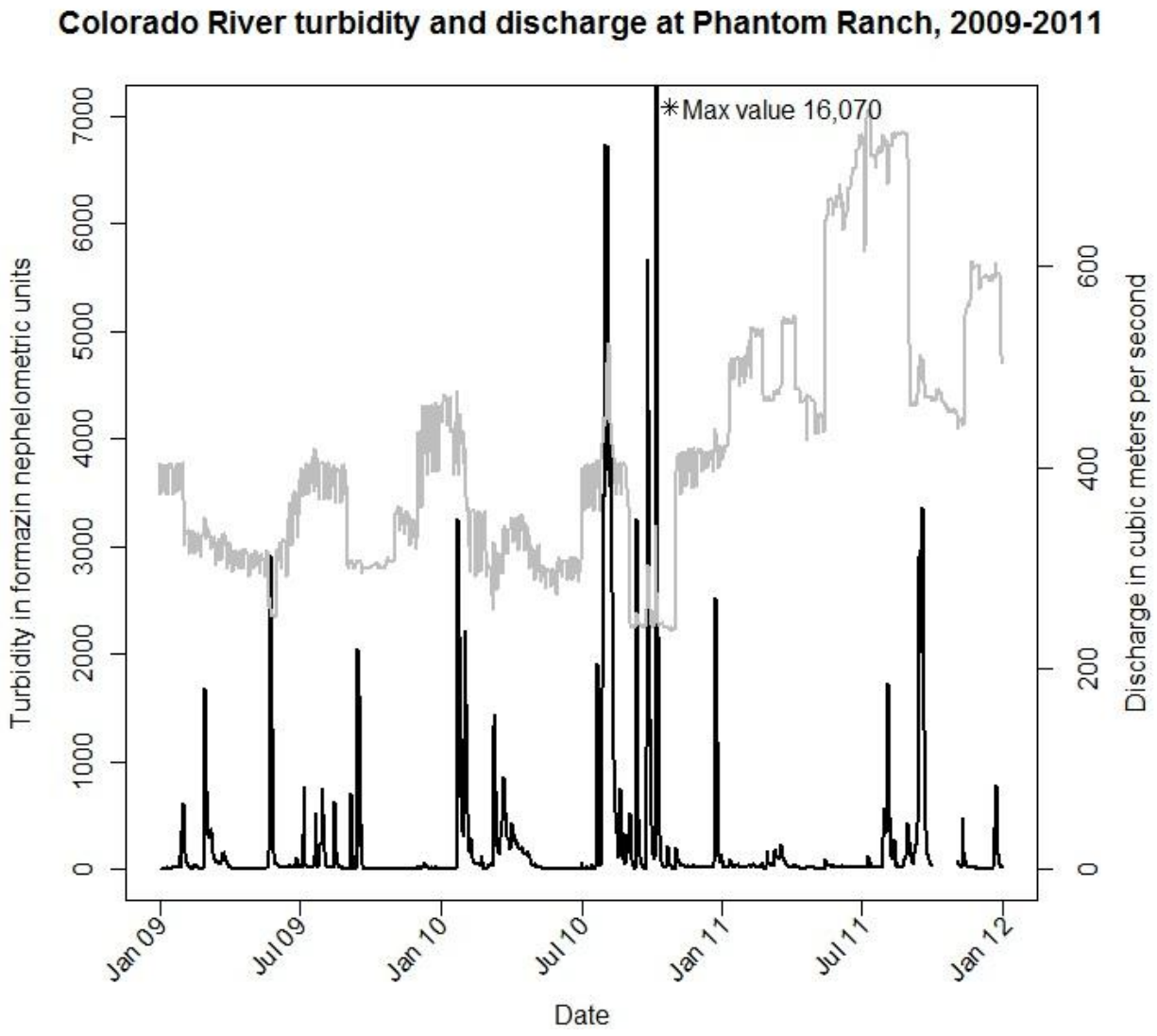

Figure 3. Colorado River turbidity (black line) and discharge (grey line) as measured at Phantom Ranch, Grand Canyon National Park, Colorado River, during the NSE sampling period 2009-2011. In each year NSE sampling trips took place in July, August, September and October.

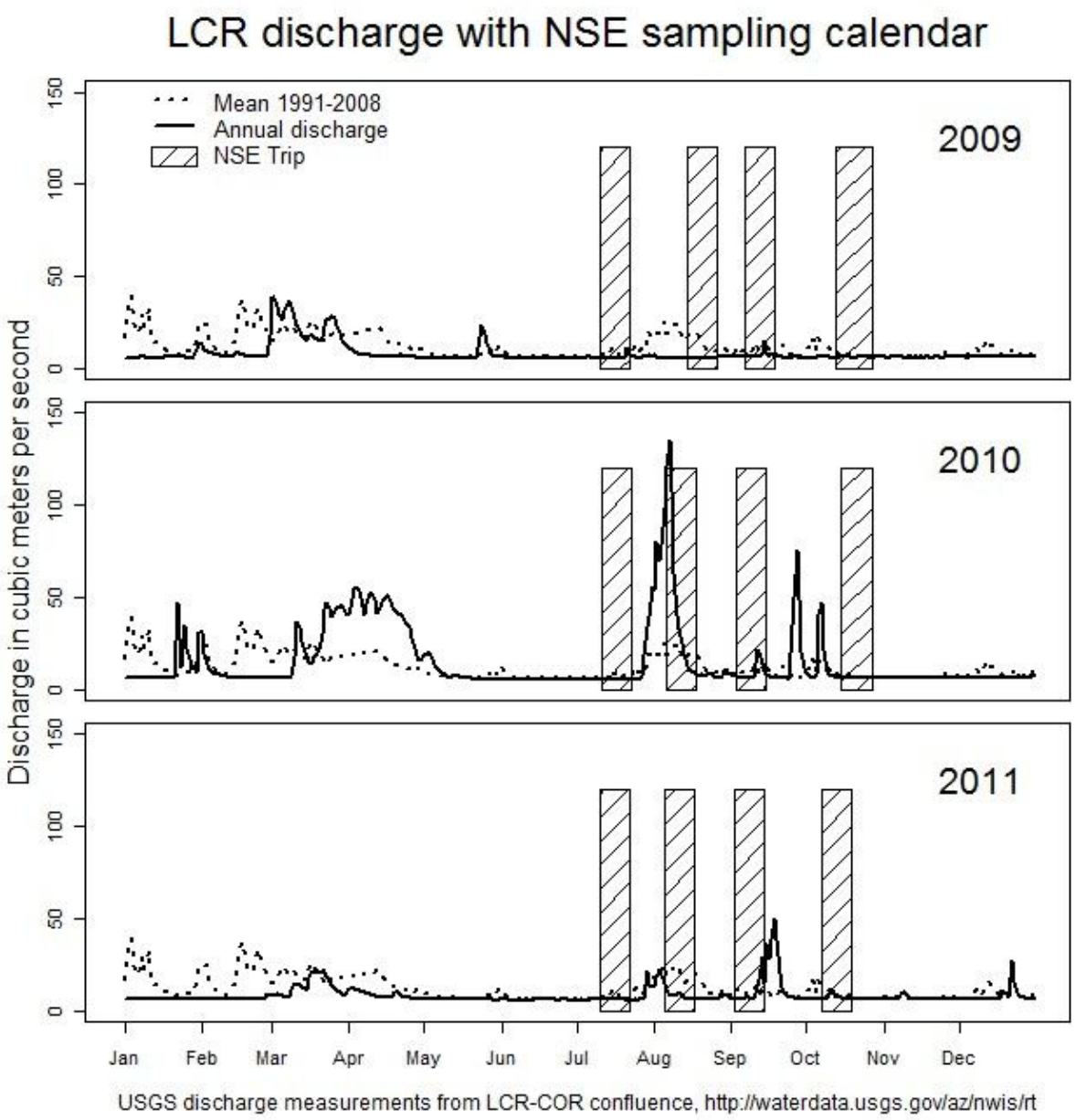

Figure 4. Discharge (m^3/sec) measurements from the Little Colorado River (LCR) - Colorado River confluence gauge, as solid black lines, for the LCR during 2009 (top panel), 2010 (middle panel), and 2011(bottom panel). The dashed black line represents the mean discharge from 1991-2008. The vertical striped rectangles represent the NSE sampling periods in the mainstream just downstream of the confluence in each year. The NSE sampling reach is heavily influenced by LCR tributary inputs in terms of influencing turbidity and also the out migration of juvenile native fish.

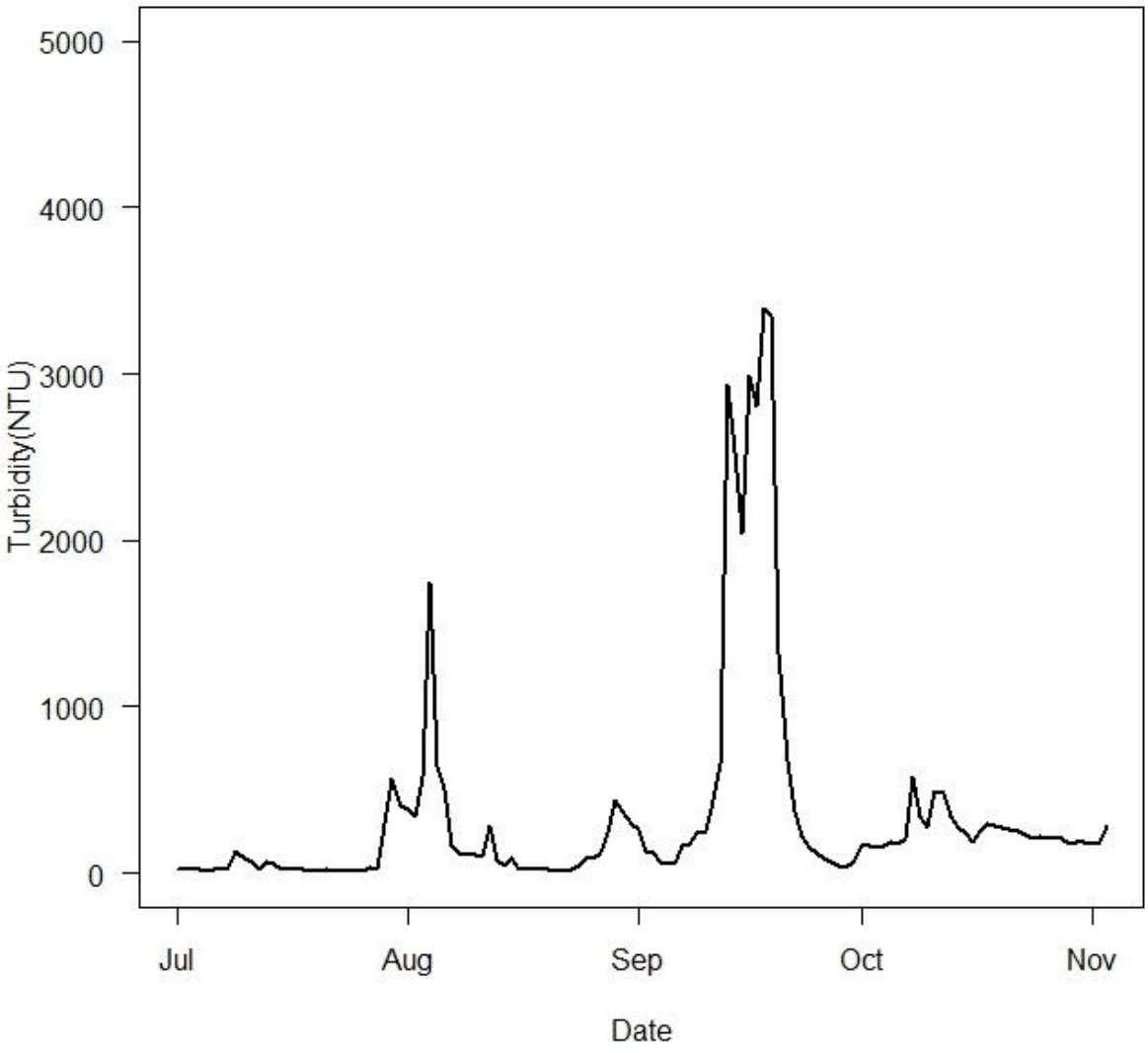

Figure 5. Turbidity (NTU) measured at Phantom Ranch during summer 2011 and travel time corrected to approximate the turbidity values at the NSE sample sites between Heart Island and Lava Chuar rapid. NSE sampling trips in 2011 launched in mid-July, mid-August, early September and mid-October.

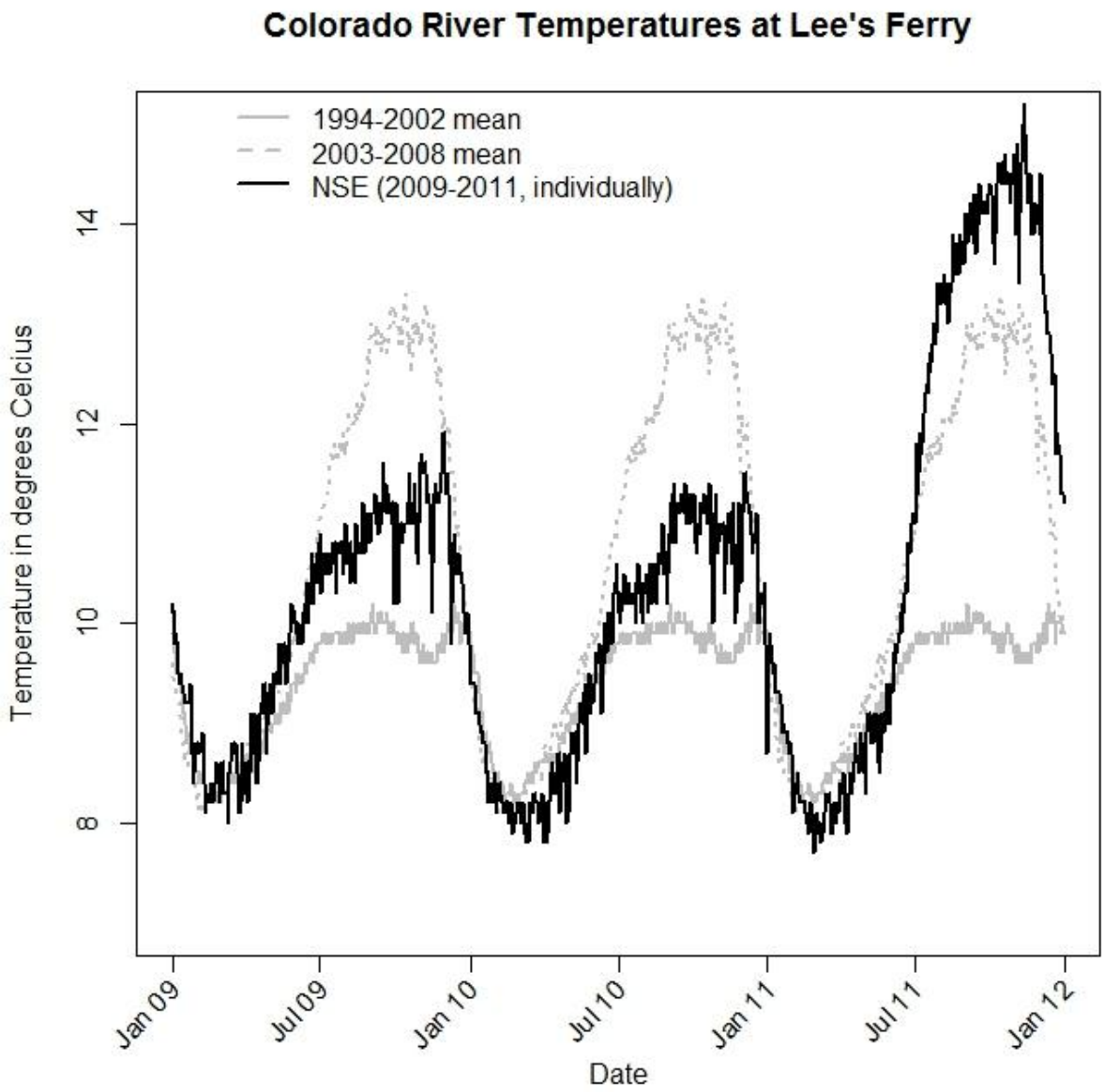

Figure 6. Water temperature (°C) in the Colorado River measured at Lee's Ferry. The solid grey line is the 1994-2002 mean temperature. The grey dotted line is the 2003-2008 mean temperature, a period of warm water related to low reservoir levels. The solid black line is the water temperature in each year (x-axis) of the NSE project. Note that 2011 was the warmest NSE project sampling year.

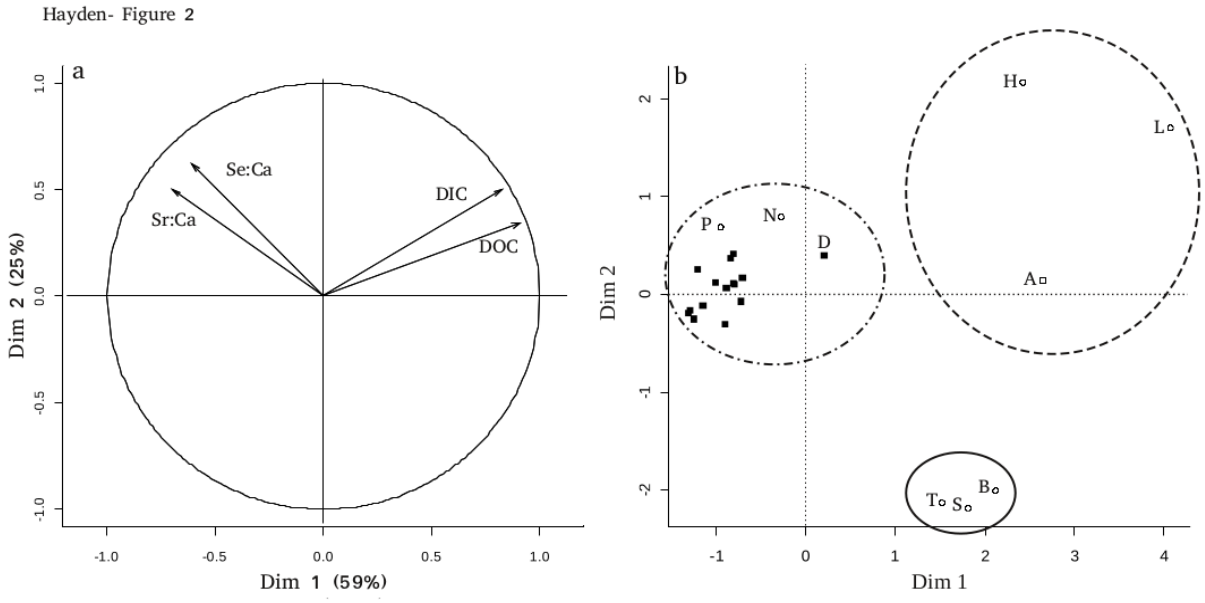

Figure 7. Multivariate principal component analysis of Colorado River and tributary water chemistry in the Grand Canyon. Water Sr:Ca, Se:Ca, DOC $\delta^{13}C$, and DIC $\delta^{13}C$ were quantified. Samples were collected in October 2009. Variable loadings (a) and Bi-plot (b) of the first two principal components. Solid squares represent samples collected in the Colorado River, open circles are tributary samples, and the open square is the spring sample. Circles depict sample sites with similar chemistry (solid = Bright Angel Creek, Tapeats Creek, and Shinumo Creek, dashed = Little Colorado River, Havasu Creek, and 30-Mile Spring, dot-dashed = Colorado River, Paria River, Diamond and Nankoweap creeks). *Note figure is part of a manuscript currently under review in River Research and Management*

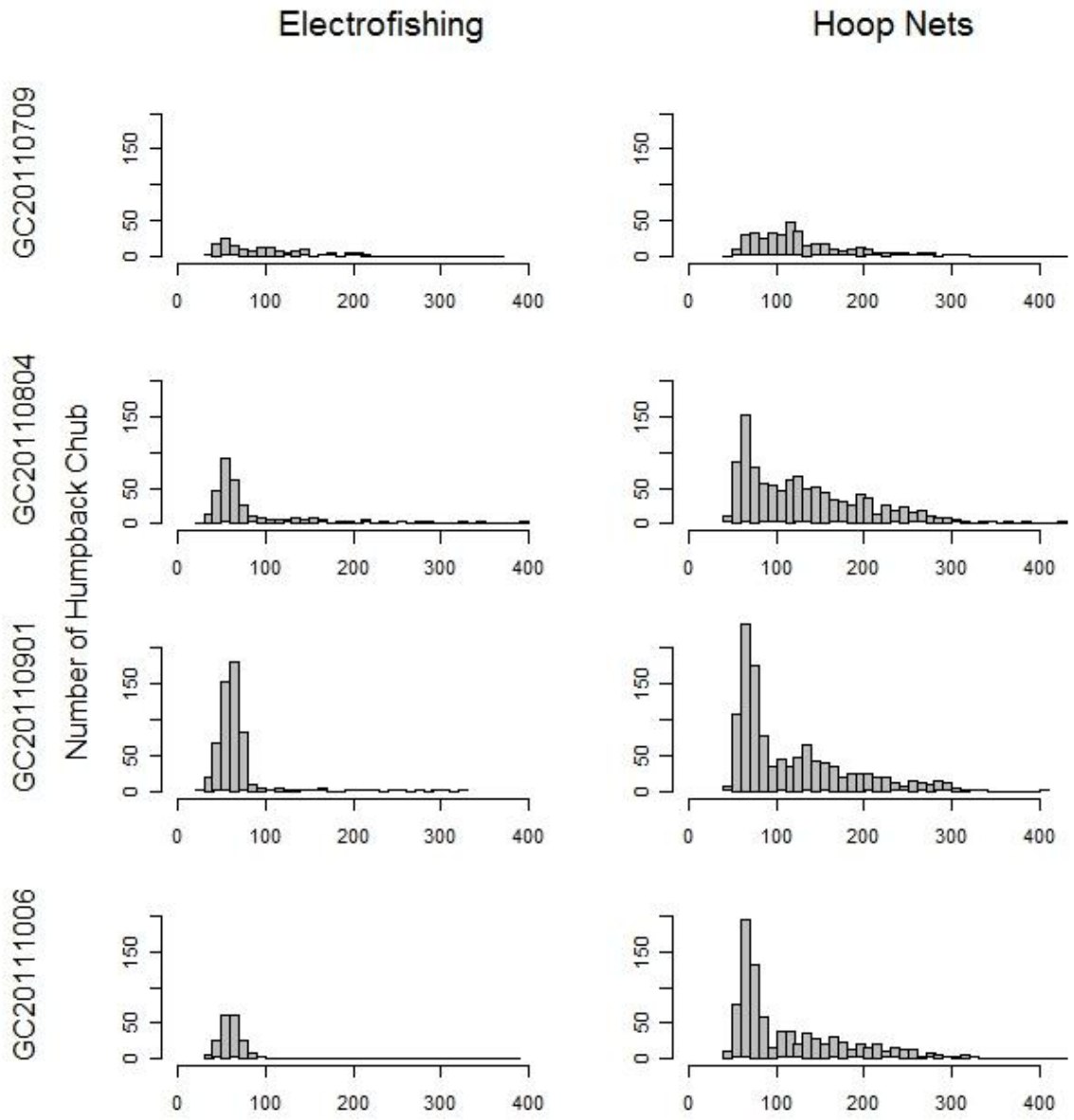

Figure 8. Length (mm TL, x-axis) frequency distributions of humpback chub collected during 2011 NSE sampling trips (each row) by electrofishing (left column) and hoop nets (right column).

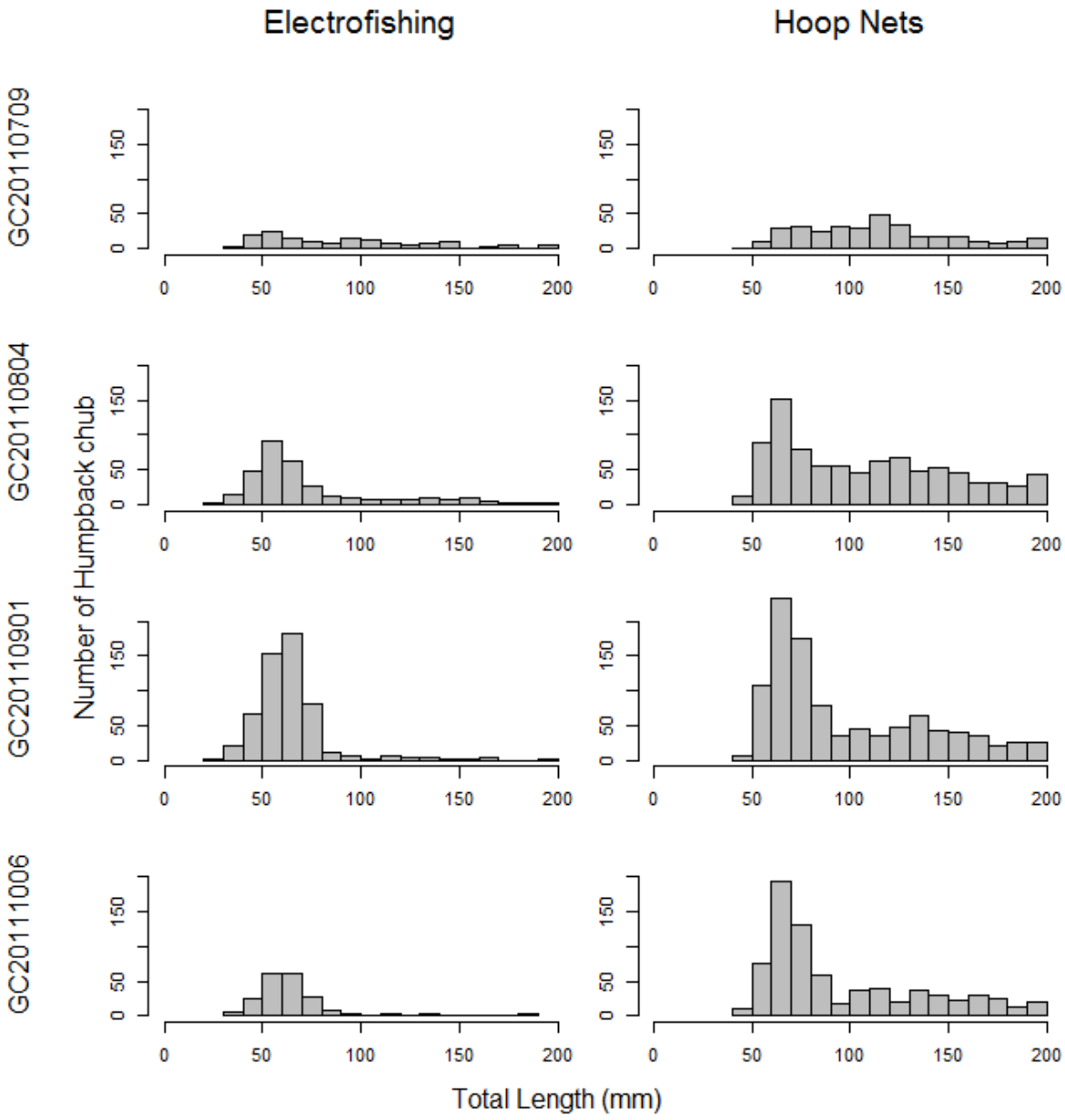

Figure 9. Length (mm TL, x-axis) frequency distributions of humpback chub collected during 2011 NSE sampling trips (each row) by electrofishing (left column) and hoop nets (right column). This is the same figure as Figure 8, but the X-axis is truncated at 200-mm to make it easier to see the size structure of small fish collected in each gear.

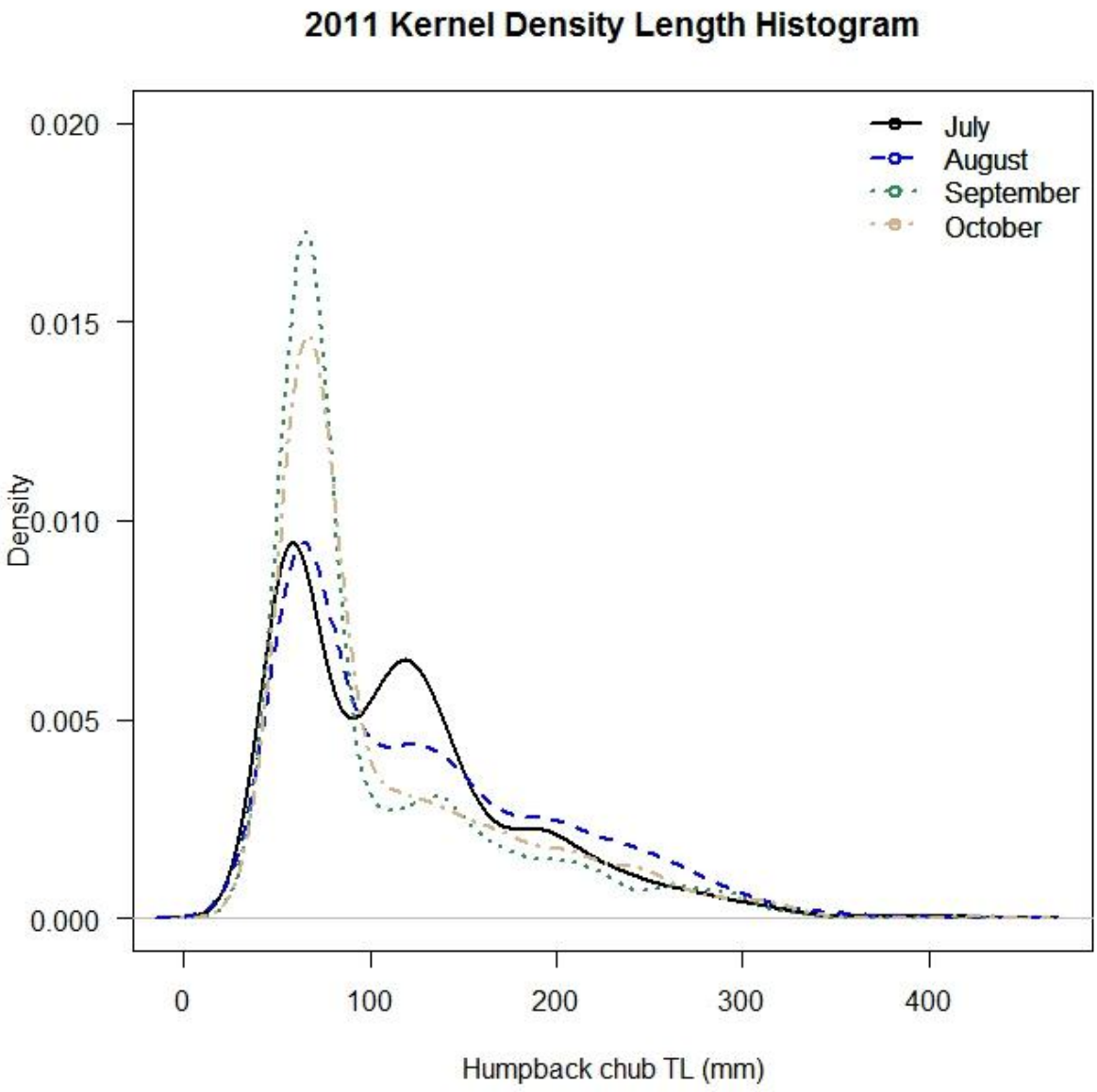

Figure 10. Kernel density histogram of humpback chub total length (mm TL) collected across each NSE sampling trip (July-October) in the mainstem Colorado River.

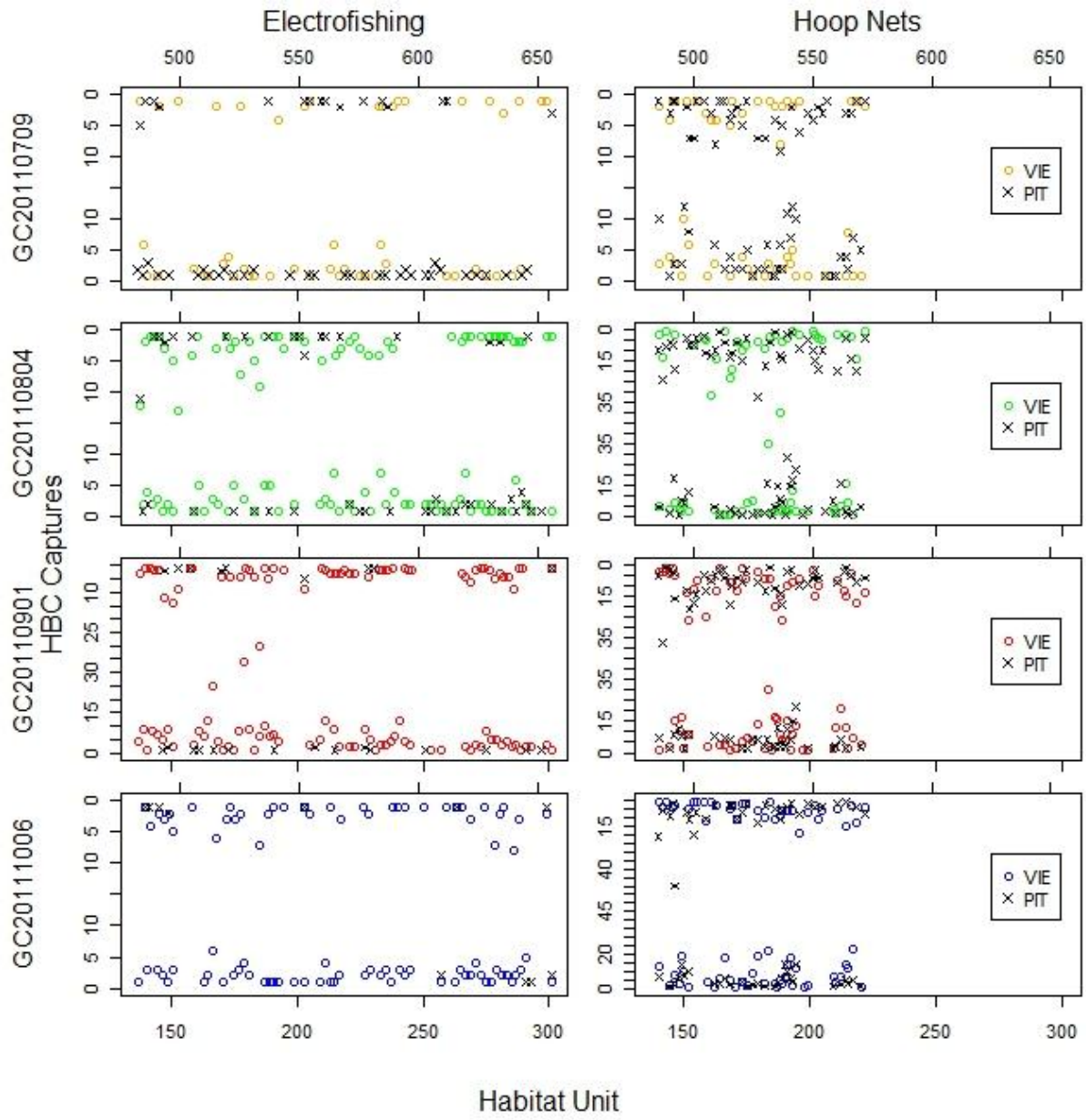

Figure 11. Spatial distribution of juvenile (<200-mmTL) humpback chub catch by HSU in 2011. HSUs from river right (sites 140-300) are found on the primary x-axis and the HSUs for river left (sites 450-650) are found on the secondary x-axis. The catch in each of these grid cells (y-axis) then correspond to each x-axis such that catches close to zero for a given HSU are near the axis corresponding to that HSU (either primary or secondary x-axis) and non-zero catches are a greater distance away from the corresponding x-axis. VIE marked HBC (<100-mm TL) are indicated with a circle and PIT tagged fish (100-mm TL) are indicated with an X

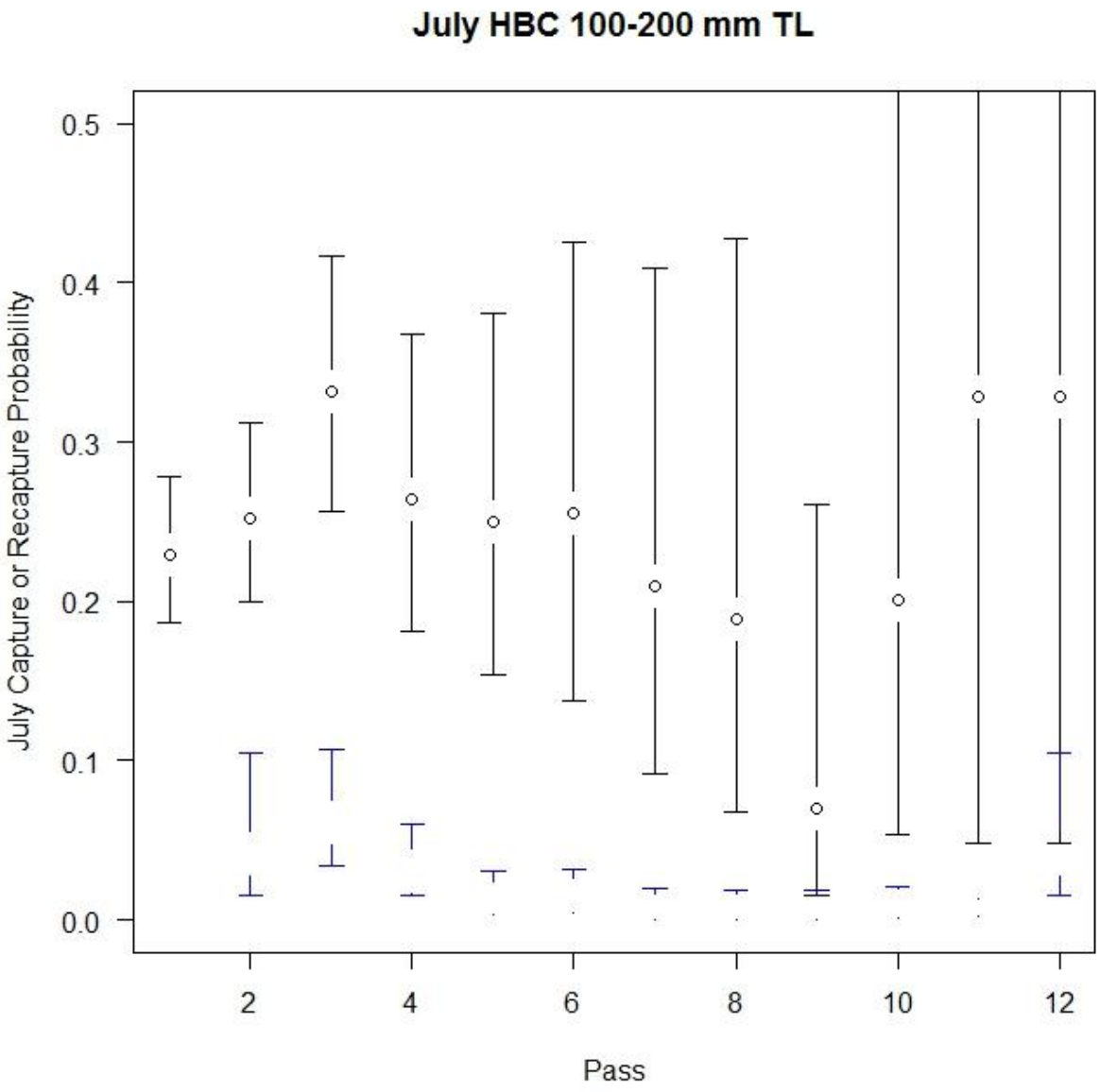

Figure 12. Representative capture probabilities (p-hat, black lines) and recapture probabilities (blue lines) of humpback chub from two size categories collected during the NSE project across pass for July 2011 from a model with time dependent capture and recapture probability. Error bars represent approximate 95% confidence intervals.

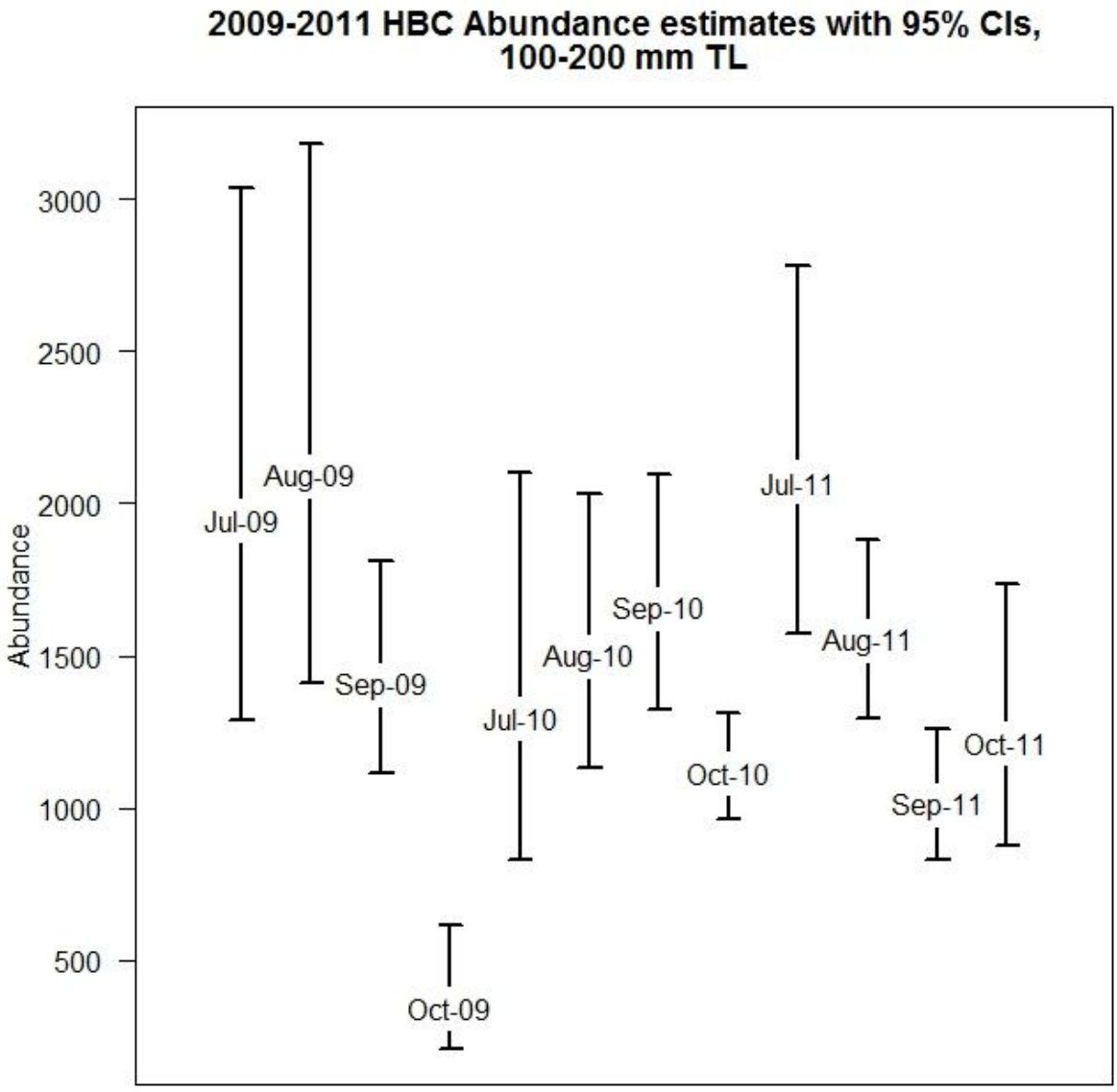

Figure 13. Estimated abundance of juvenile humpback chub from 100-200-mm TL from each NSE sampling trip during 2009-2011. Error bars represent approximate 95% confidence intervals. We are currently refining analytical approaches used to estimate abundance and will have revised estimates available in summer 2012.

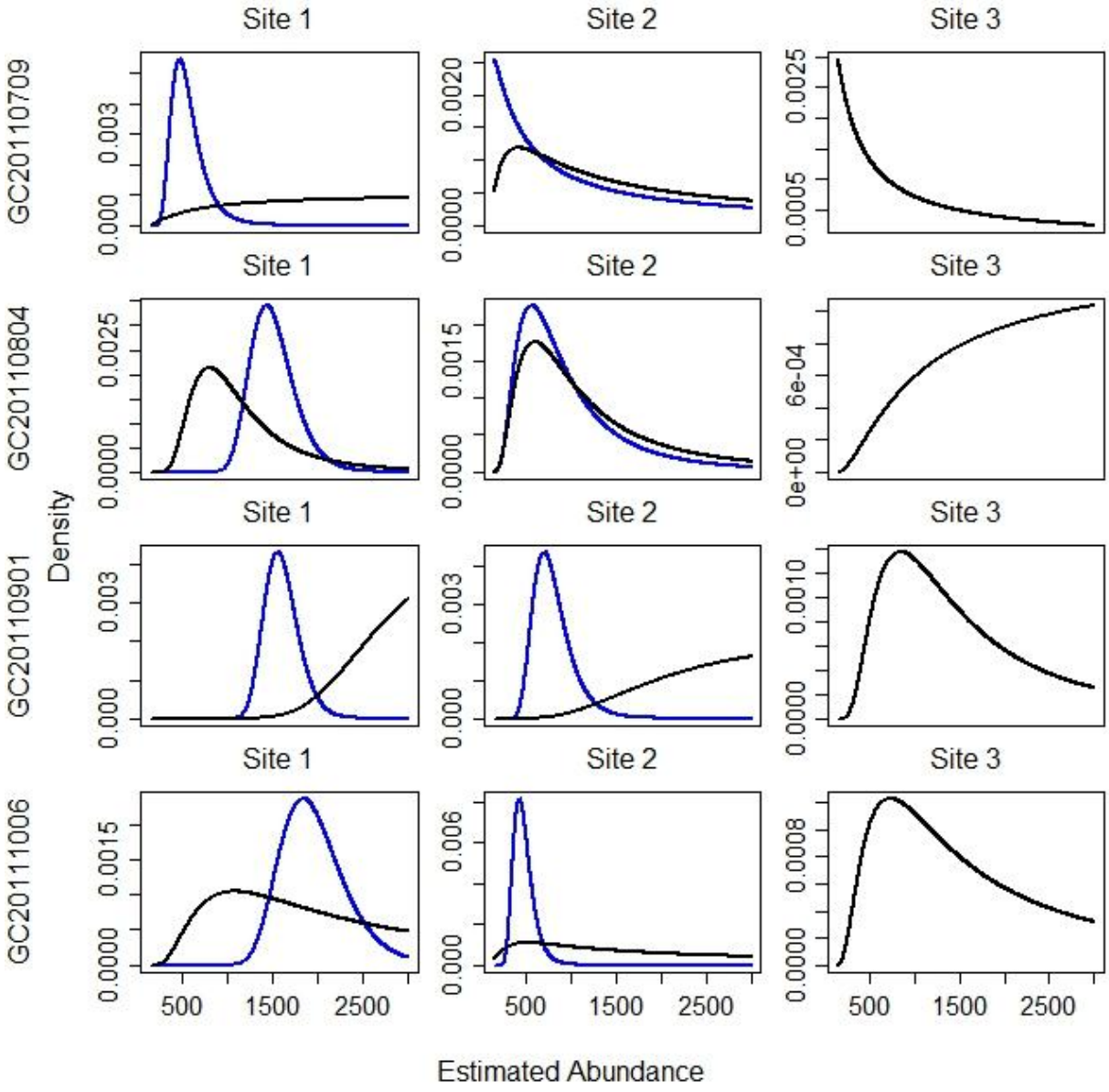

Figure 14. Profiles of abundance estimates of humpback chub <100-mm TL abundance in each NSE sampling site (columns) for each trip (rows) during 2011 using closed population abundance methods from Gazey and Staley (1986). Estimates in Site 1 (left column) and Site 2 (middle column) were made using both electrofishing (black line in all plots) and hoopnets (blue line) while only electrofishing was used in Site 3.

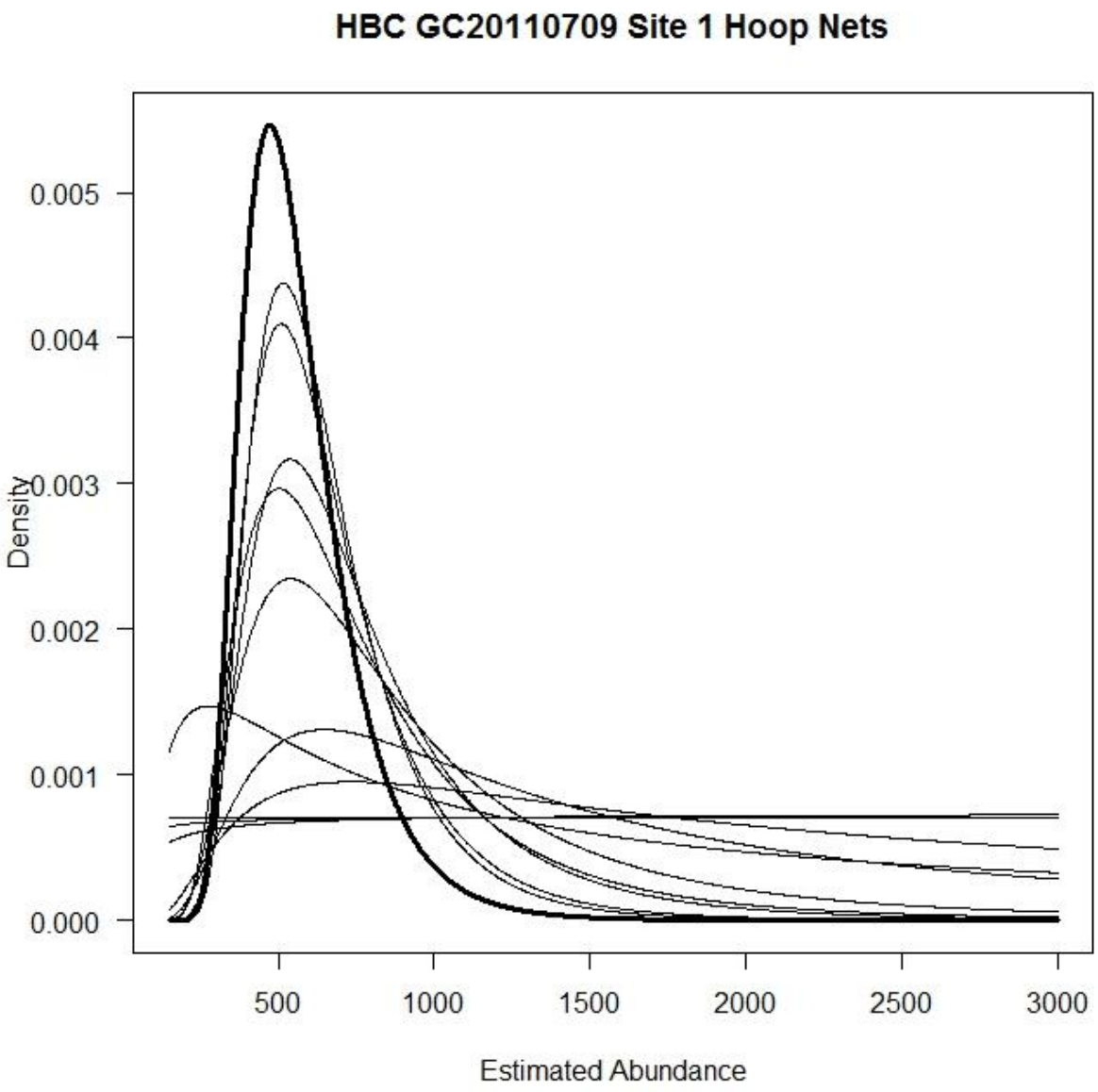

Figure 15. Likelihood estimates of humpback chub <100-mm TL abundance from hoopnetting data collected for Site 1, Trip 1 in 2011. Thick black line represents the maximum likelihood estimate (MLE) of abundance after 12 nights of hoopnet sampling while the thin horizontal lines represent the (unconverged) likelihood estimate of abundance after each sequential night of sampling. In general a minimum of 7 nights of hoopnetting were required before a credible (i.e., dome shaped) estimate of abundance were made. With increasing samples (nights of fishing) likelihood estimate becomes better defined and resulting MLE is plotted as the think black line.

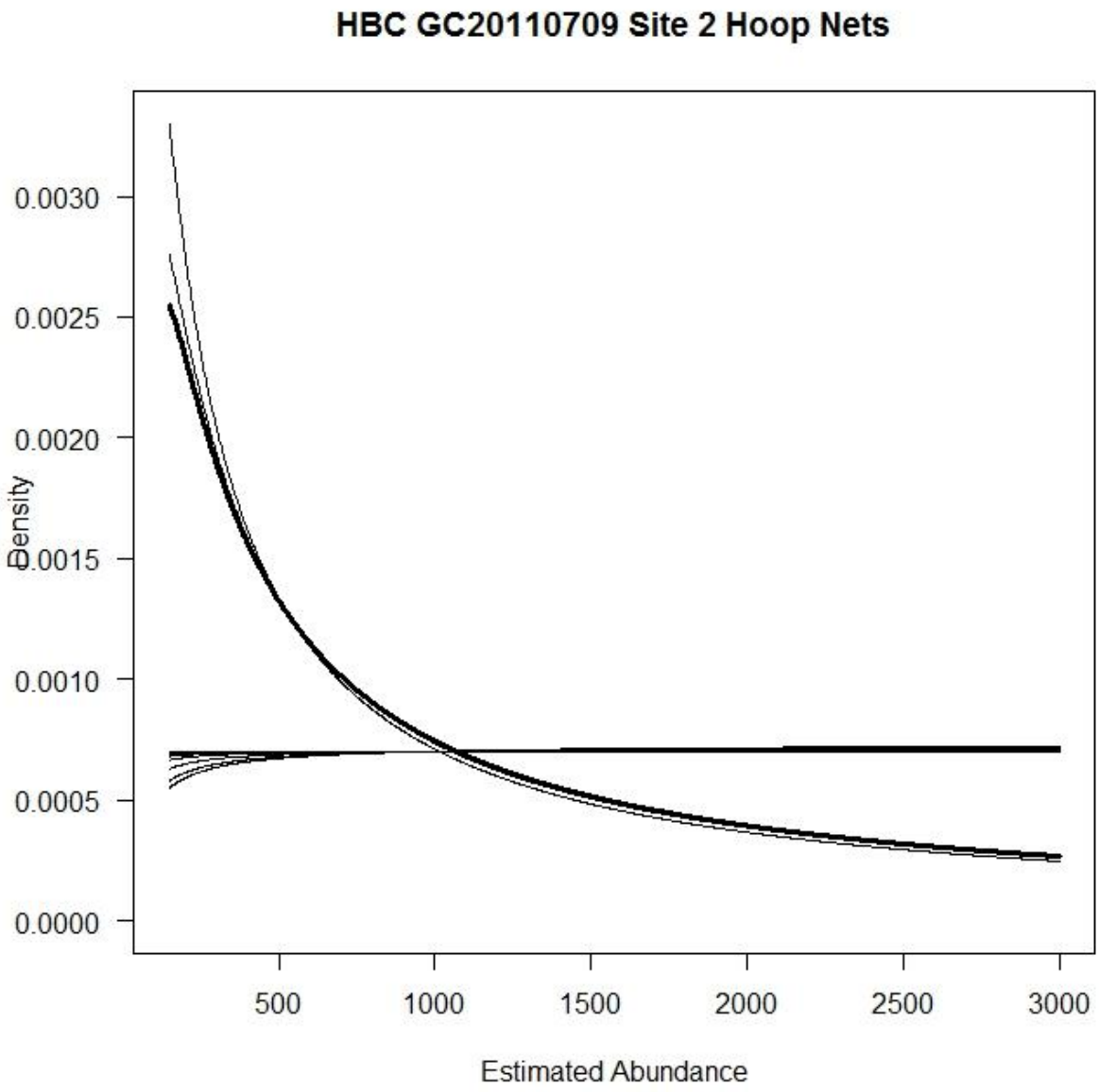

Figure 16. Likelihood estimates of humpback chub <100-mm TL abundance from hoopnetting data collected for Site 2, Trip 1 in 2011. This is the same type of plot as the previous but in this sampling month at this site, convergence was not reached because of sparse recaptures so no credible abundance estimate was made.

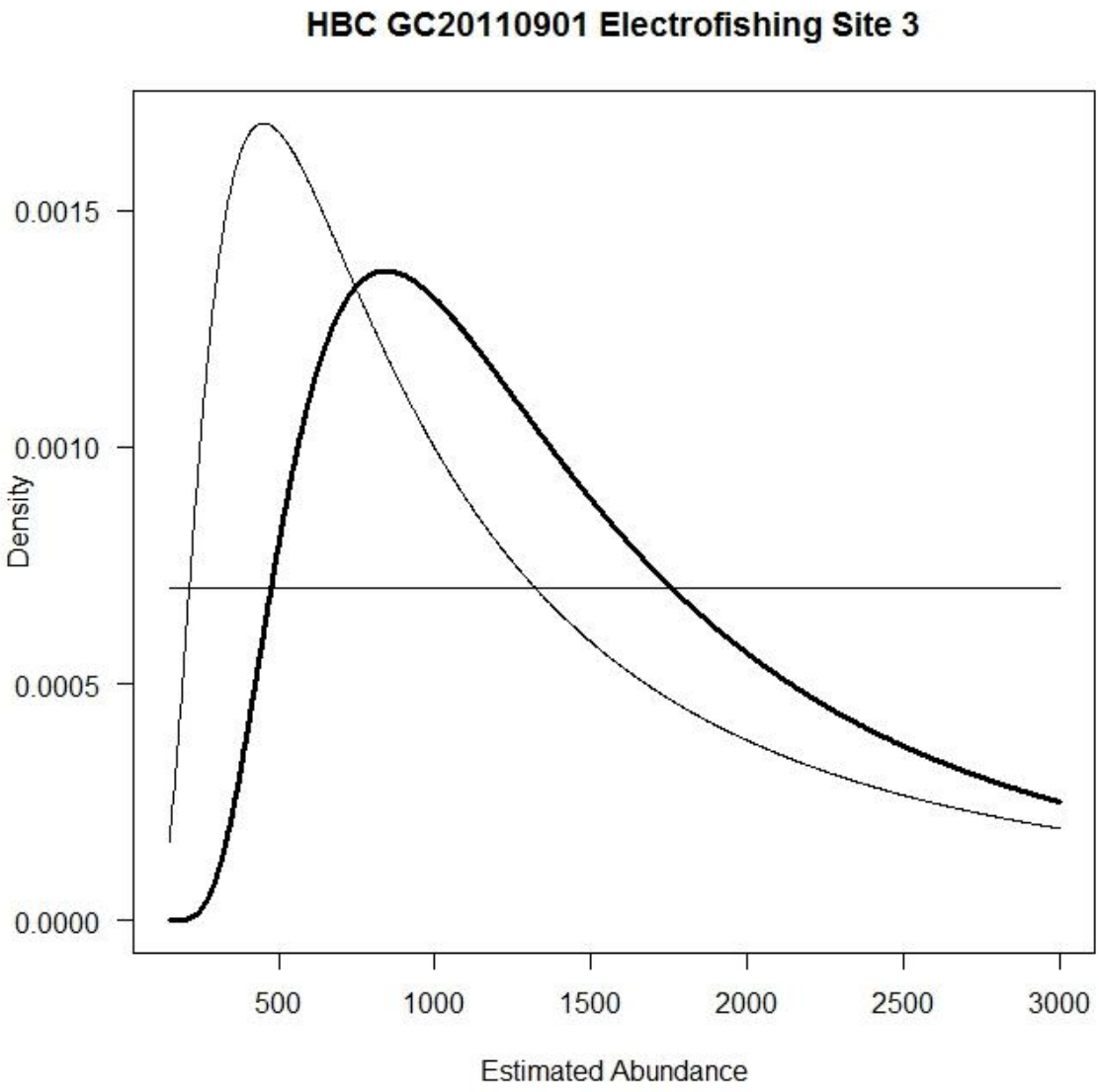

Figure 17. Example likelihood estimates of humpback chub <100-mm TL abundance from electrofishing data collected for Site 1, Trip 1 (20090709). Thick black line represents the maximum likelihood estimate (MLE) of abundance after three electrofishing passes while the thin horizontal line represents the (unconverged) likelihood estimate of abundance after 1 pass while the thin dome shaped line with the long tail represents the likelihood estimate after 2 electrofishing passes.

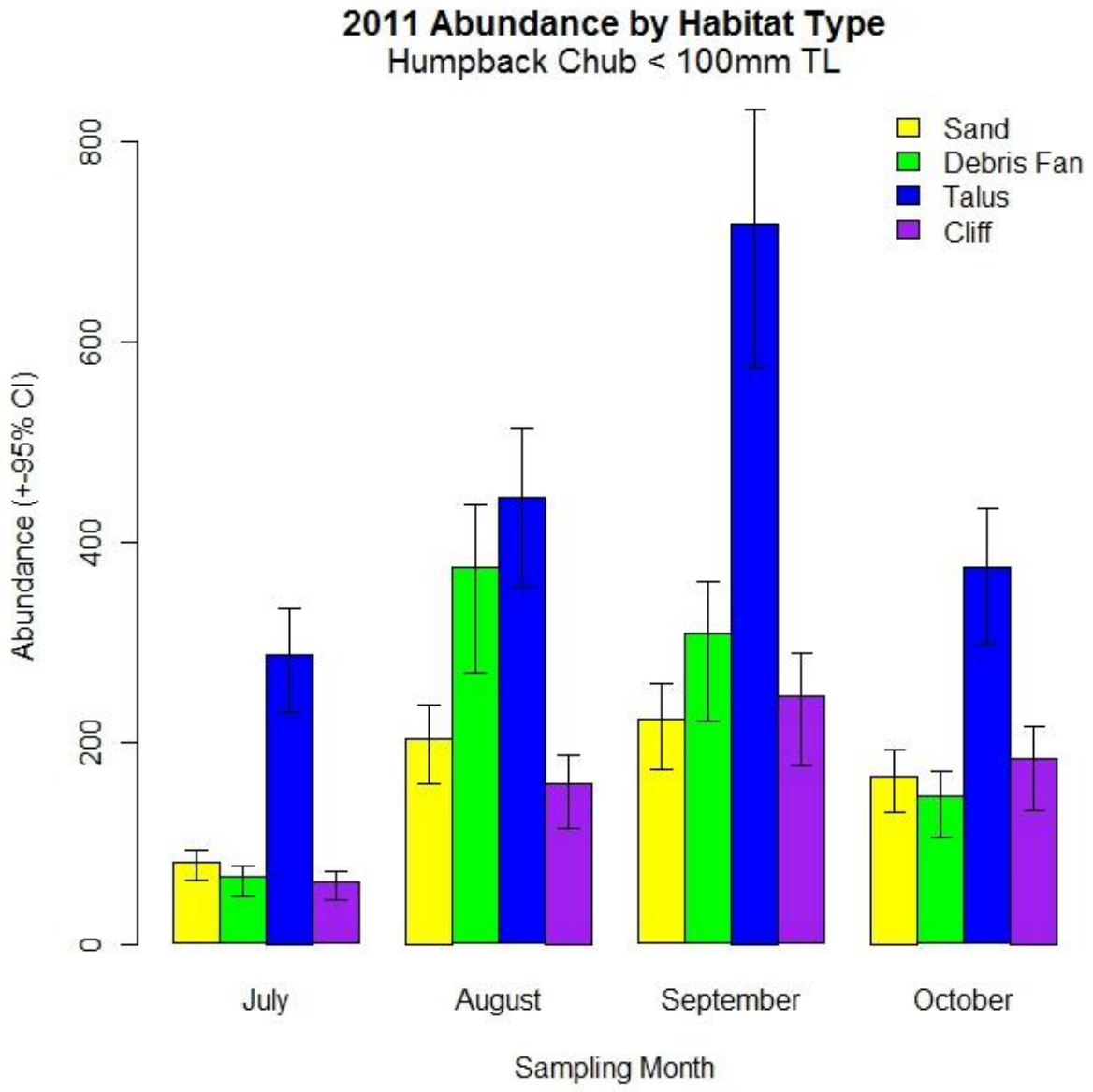

Figure 18. Example figure of HBC <100-mm TL abundance estimated by habitat type. Here we estimated habitat specific capture probabilities based on marks and recaptures of fish in a specific habitat type, then divided the catch in that habitat type of the capture probability. Uncertainty was estimated via bootstrap resampling of the capture probability estimates from each HSU within a habitat type. This approach of sharing information on capture probability across a spatial covariate such as habitat type, instead of an arbitrary spatial unit like site is an example of the type of approaches we will assess in 2012 to determine the best approach to estimating abundance.

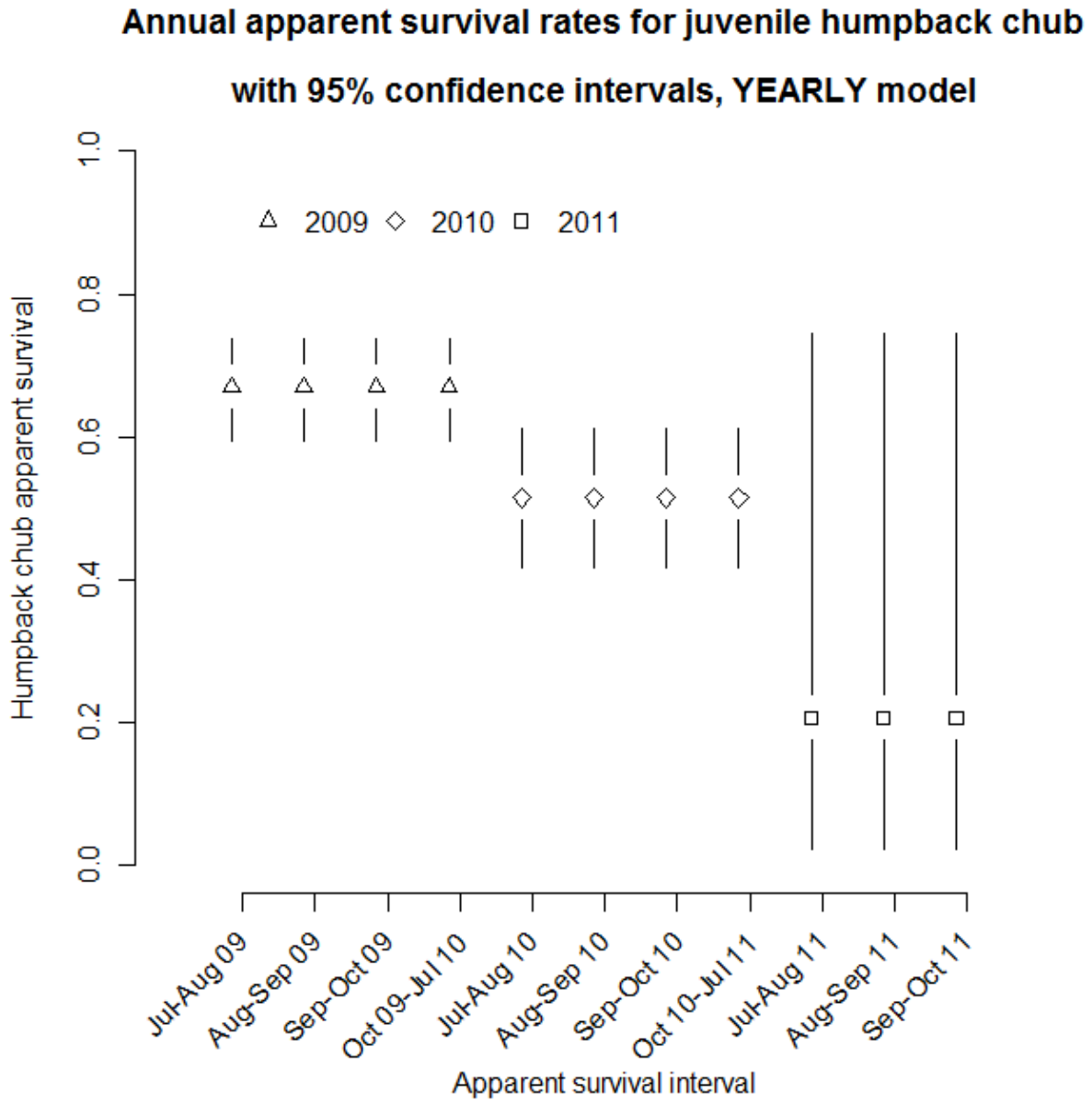

Figure 19. Annual apparent survival rates from the leading model, which calculated them independently for each year. Quantitative support for this annual model as described by Akaike's Information Criterion corrected for small samples sizes (ΔAICc) is differentiated by less than three points from the next two models, which are flow-based models.

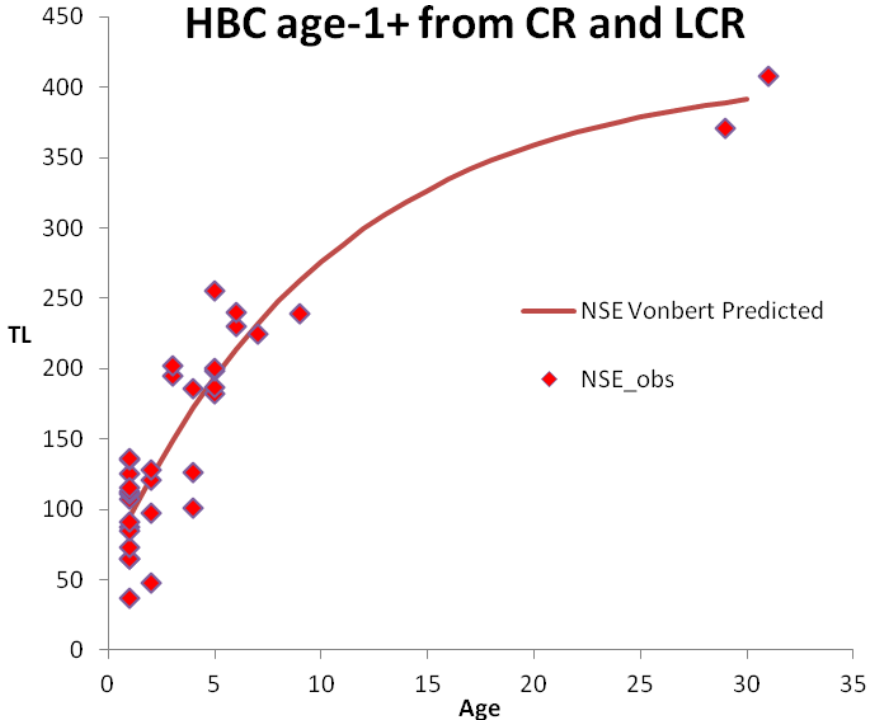

Figure 20. Preliminary age (x-axis, years) vs. length (TL, mm, y-axis) for humpback chub aged by the NSE project from incidental mortalities or fish found dead by the NSE team or other agency cooperators. The red line is a vonBertalanffy growth curve fit to the data.

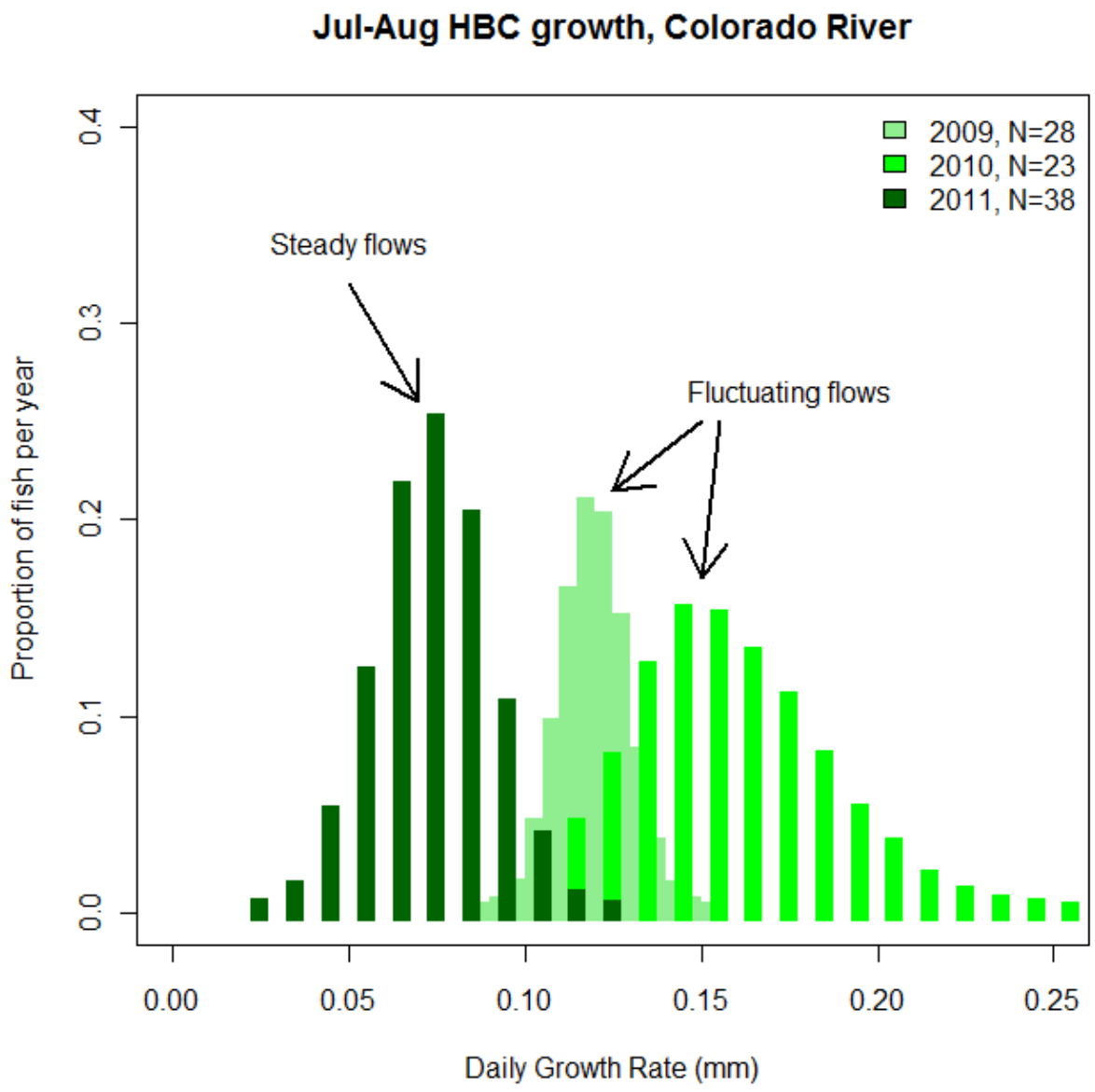

Figure 21. Daily growth rate (mm) of juvenile humpback chub in the mainstem Colorado River during summer periods (July-August of 2009-2011). Summer 2011 provided a crucial contrast as a steady flow period (summer 2009 and 2010 were during modified low fluctuating flow regimes), yet demonstrated lower daily growth rates in juvenile humpback chub. Distributions represent approximate 95% bootstrap confidence intervals.

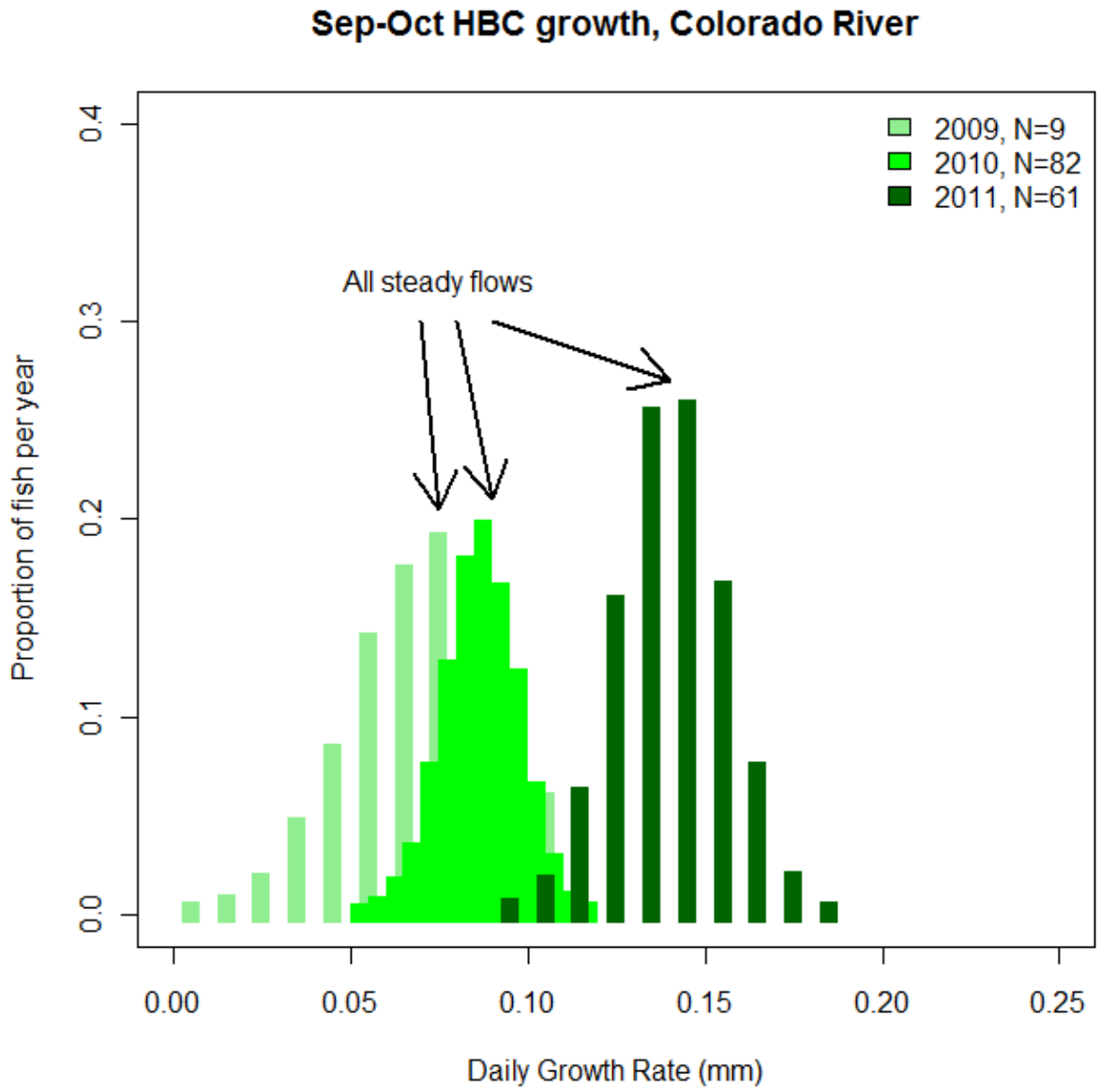

Figure 22. Daily growth rate (mm) of juvenile humpback chub in the mainstem Colorado River during fall periods (September-October of 2009-2011). Higher growth in fall 2011 is noteworthy as a contrast to lower growth in summer 2011 (Figure 22). Distributions represent approximate 95% bootstrap confidence intervals.

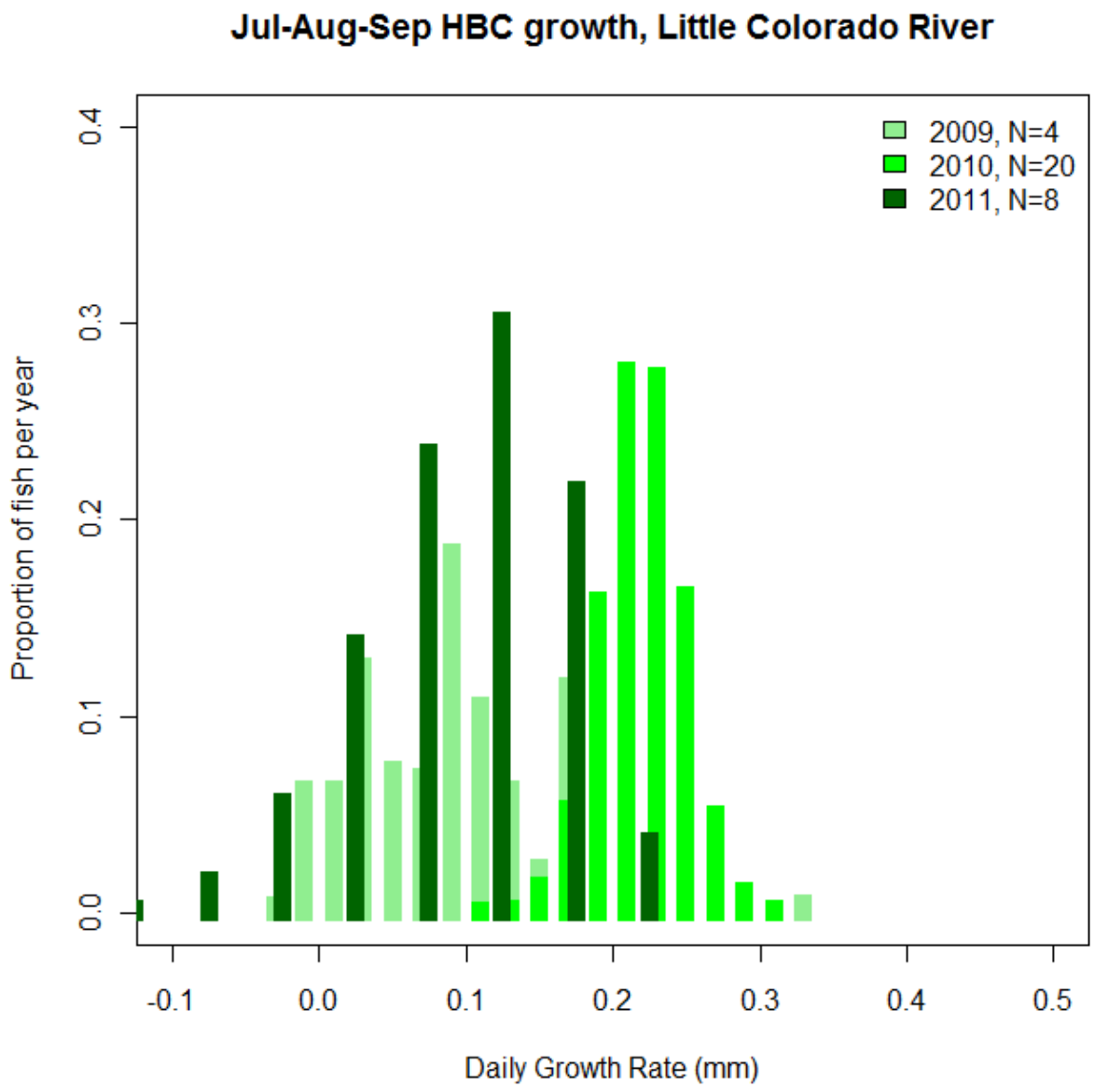

Figure 23. Daily growth rate (mm) of juvenile humpback chub in the Little Colorado River during summer (July to August or early September). Distributions represent approximate 95% bootstrap confidence intervals.

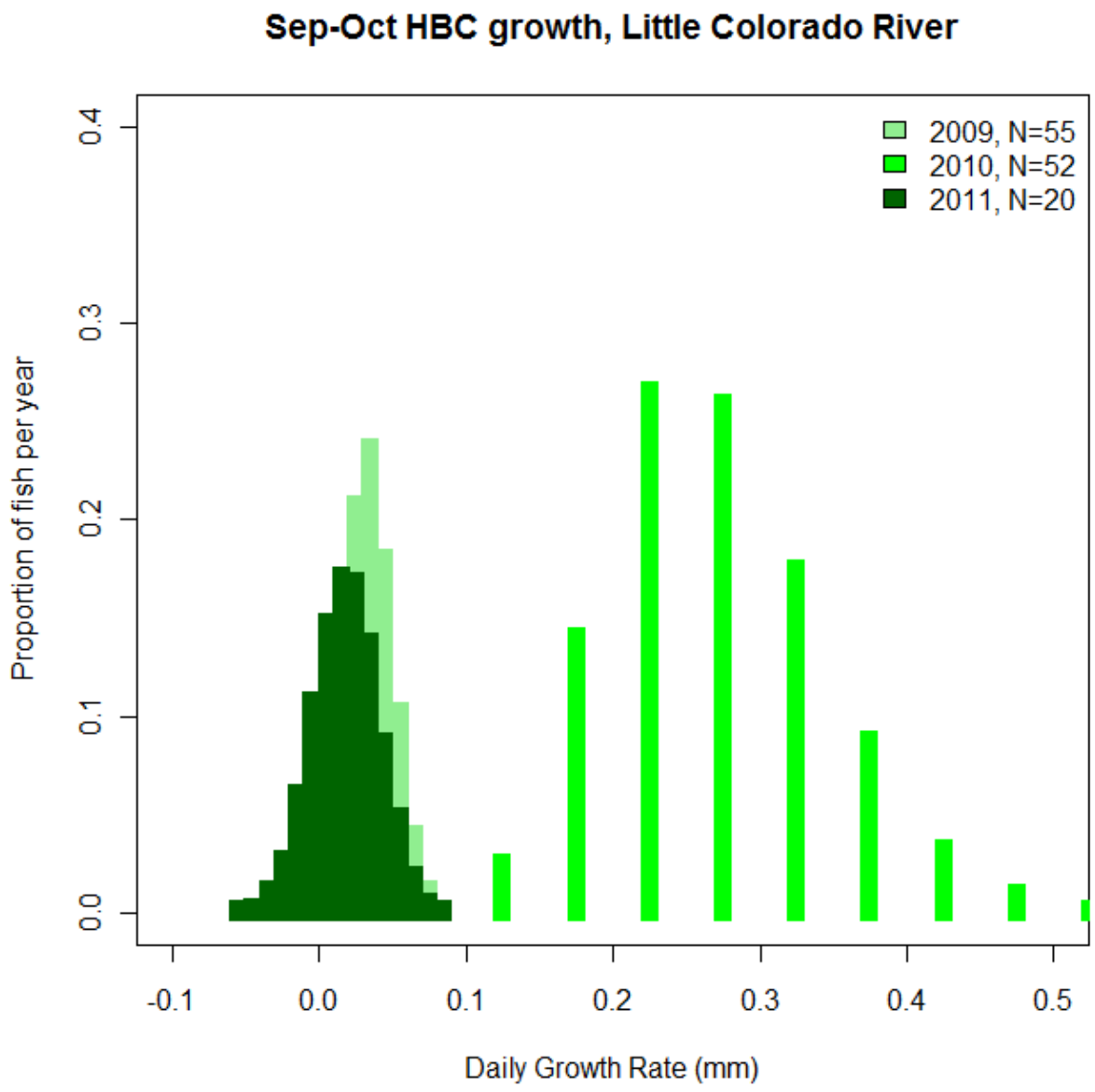

Figure 24. Daily growth rate (mm) of juvenile humpback chub in the Little Colorado River during fall periods (September to October) in each year of the NSE study. Distributions represent approximate 95% bootstrap confidence intervals.

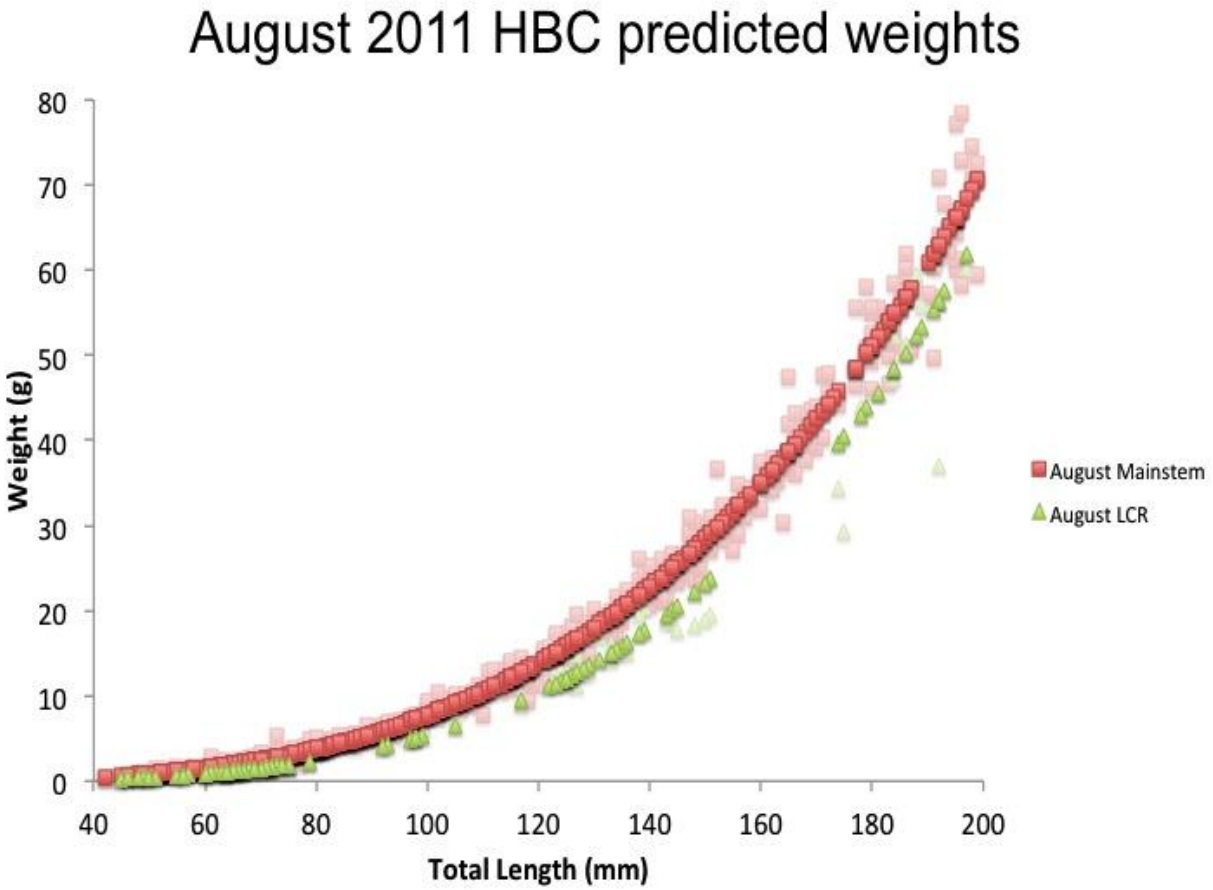

Figure 25. Comparison of predicted weight of juvenile humpback chub in the mainstem Colorado River and Little Colorado River during August of 2011. Weights are predicted using the equation $W=aL^b$ (where *W* is fish weight in grams, *L* is fish length in mm and *a* and *b* are model parameters).

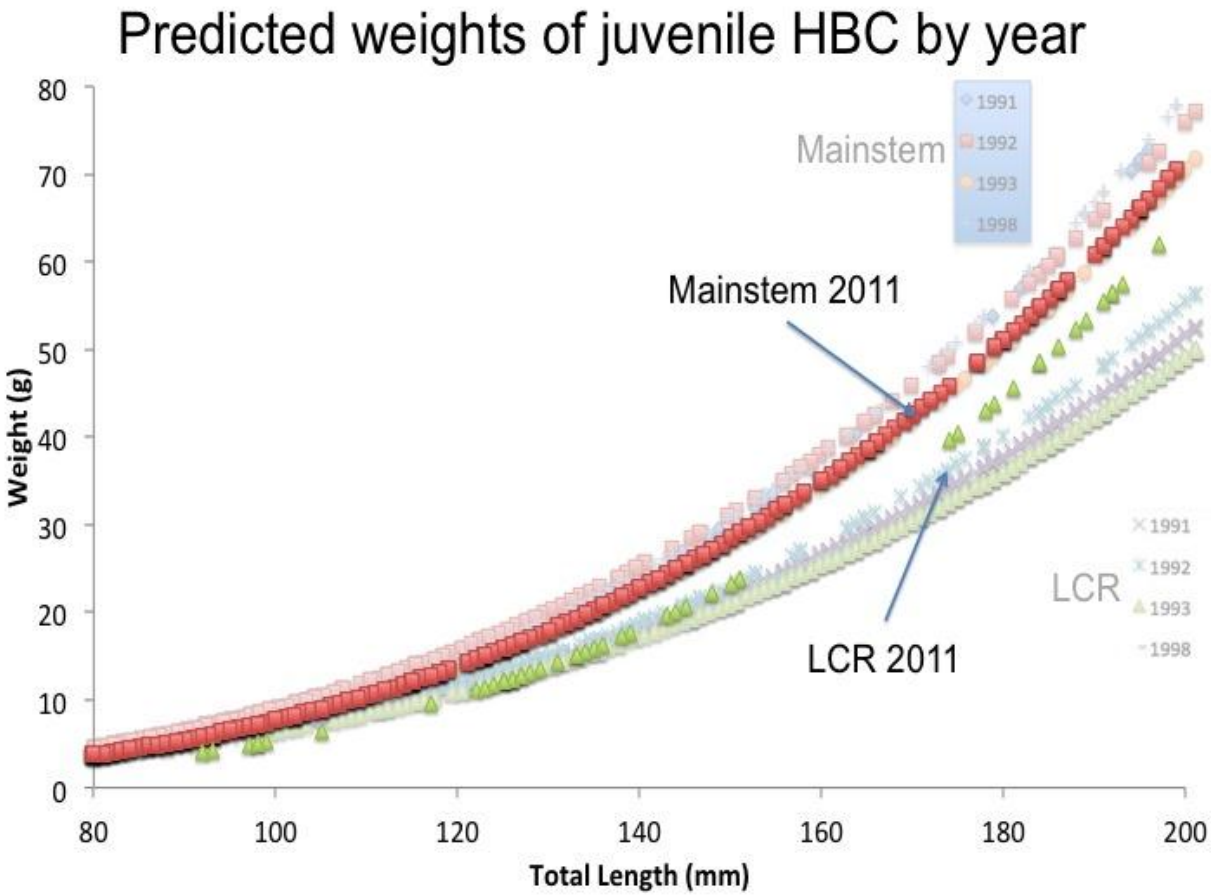

Figure 26. Comparison of predicted weight of juvenile humpback chub during August for all five years with available data from the mainstem Colorado River and Little Colorado River. Weights are predicted using the equation $W=aL^b$ (where *W* is fish weight in grams, *L* is fish length in mm and *a* and *b* are model parameters).

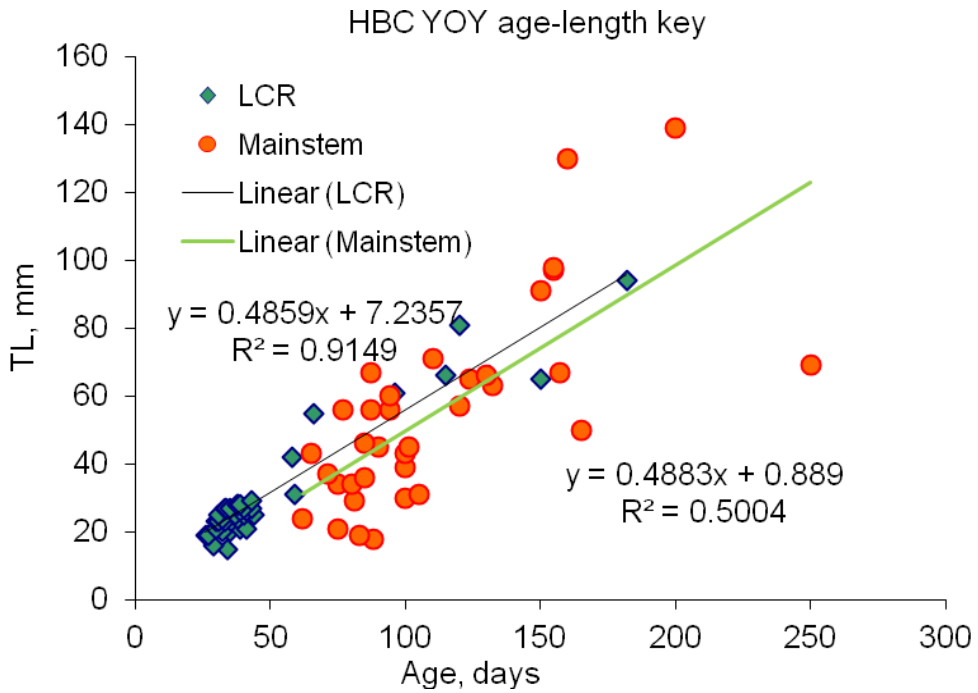

Figure 27. Preliminary age (x-axis, days) vs. length (TL, mm, y-axis) for juvenile humpback chub collected in the LCR (diamonds) or mainstem circles). Linear regressions are fit to the two data sets with the LCR ($y=0.4859x + 7.2357$, $R^2=0.9149$) a better linear fit than data from the mainstem ($R^2=0.5004$).

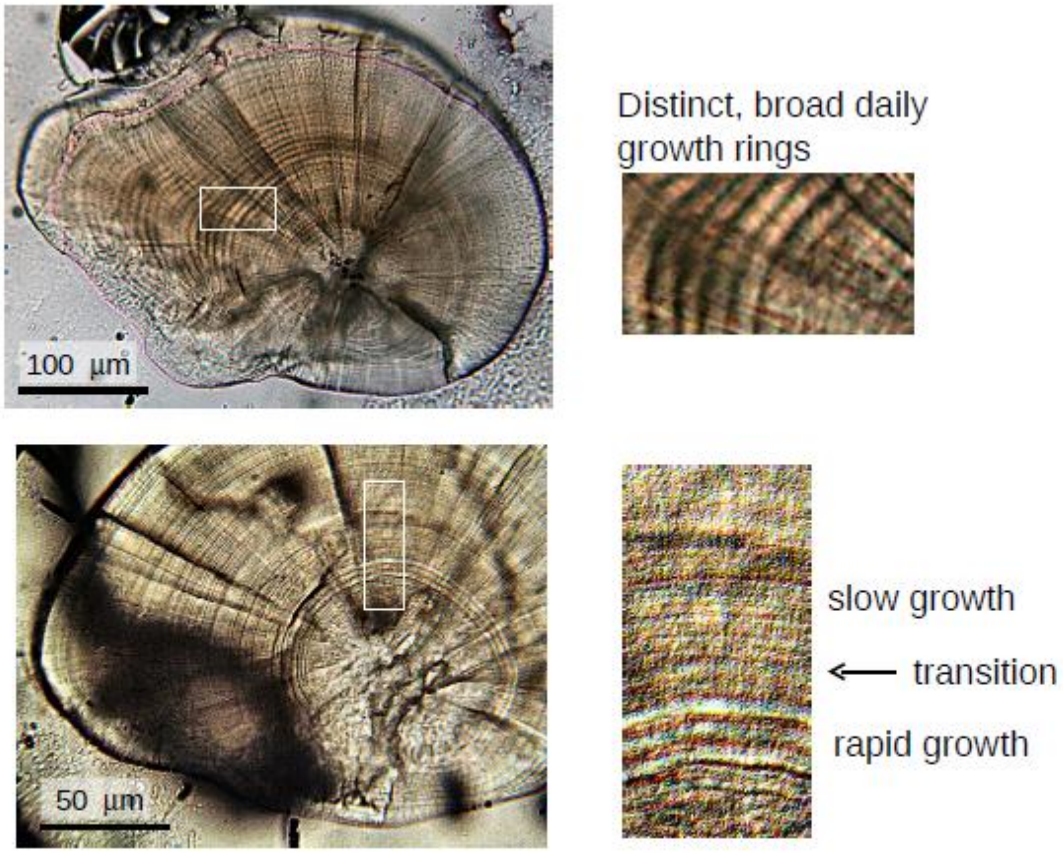

Figure 28. Example micrographs of otoliths of juvenile humpback chub from a manuscript submitted for review in *River Research and Applications*. Top: Fish-7, captured June 1, 2010 in the Little Colorado 3 km above the confluence with the mainstem, 28 mm, 39 days old. Bottom: Fish-3, captured September 4, 2006 at river km 48.5 in the mainstem Colorado; this fish was only 22 mm but had 83 distinct, daily increments. Insets (from white boxes to the right of the otolith images show details of ring structure. In Fish-3, note the transition from rapid growth to slow growth.

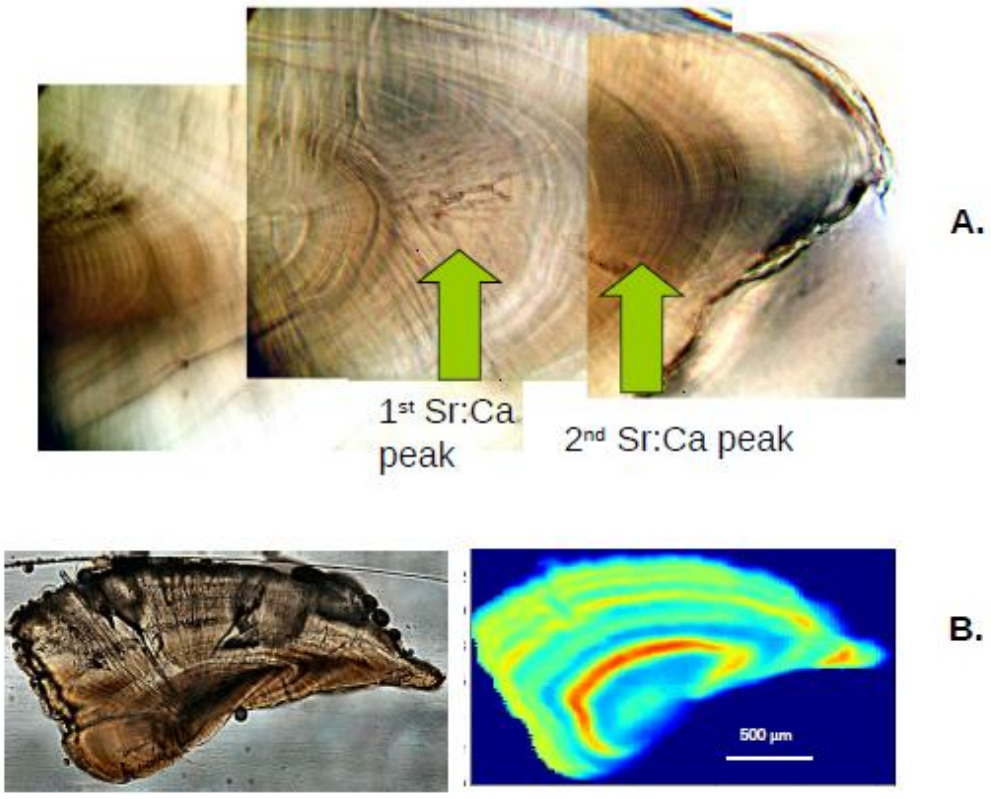

Figure 29. Example micrographs of otoliths of older humpback chub from a manuscript submitted for review in *River Research and Applications*. A: Collage of part of Fish-9 otolith, showing large rings from juvenile growth on left, followed by no visible rings where the first Sr:Ca peak occurred (winter), and subsequent visible daily increments in a period with a second, lower Sr:Ca peak (spring). This fish was 1+ years old. B. Fish-10, age 5+ years, showing otolith micrograph on left and Sr:Ca map on right. The Sr:Ca transect shown in Figure 7 was extracted from the Sr:Ca map. Sr:Ca color scale shows low values in blue and high values in red.